Homotopic affine transformations in the 2D Cartesian grid

Nicolas Passat, Phuc Ngo, Yukiko Kenmochi, Hugues Talbot

Noname manuscript No.
(will be inserted by the editor)

Homotopic Affine Transformations in the 2D Cartesian Grid

Nicolas Passat · Phuc Ngo · Yukiko Kenmochi · Hugues Talbot

Received: date / Accepted: date

Abstract Topology preservation is a property of affine transformations in $\mathbb{R}^2$, but not in $\mathbb{Z}^2$. In this article, given a binary object $\mathsf{X} \subset \mathbb{Z}^2$ and an affine transformation $\mathcal{A}$, we propose a method for building a binary object $\widehat{\mathsf{X}} \subset \mathbb{Z}^2$ resulting from the application of $\mathcal{A}$ on X. Our purpose is, in particular, to preserve the homotopy type between X and $\widehat{\mathsf{X}}$. To this end, we formulate the construction of $\widehat{\mathsf{X}}$ from X as an optimization problem in the space of cellular complexes, and we solve this problem under topological constraints. More precisely, we define a cellular space $\mathbb{H}$ by superimposition of two cellular spaces $\mathbb{F}$ and $\mathbb{G}$ corresponding to the canonical Cartesian grid of $\mathbb{Z}^2$ where X is defined, and a regular grid induced by the affine transformation $\mathcal{A}$, respectively. The object $\widehat{\mathsf{X}}$ is then computed by building a homotopic transformation within the space $\mathbb{H}$, starting from the complex in $\mathbb{G}$ resulting from the transformation of X with respect to $\mathcal{A}$ and ending at a complex fitting $\widehat{\mathsf{X}}$ in $\mathbb{F}$ that can be embedded back into $\mathbb{Z}^2$.

Keywords Affine transformations · Cartesian grid · Homotopy type · Binary images · Cubical complexes · Cellular complexes

N. Passat (corresponding author)
Université de Reims Champagne Ardenne, CReSTIC EA 3804, 51100 Reims, France
Tel: (+33) 3.26.91.33.89
E-mail: nicolas.passat@univ-reims.fr

P. Ngo
Université de Lorraine, CNRS, LORIA, France
E-mail: hoai-diem-phuc.ngo@loria.fr

Y. Kenmochi
GREYC, CNRS, Université de Caen Normandie, ENSICAEN, France
E-mail: yukiko.kenmochi@unicaen.fr

H. Talbot
Université Paris-Saclay, CentraleSupelec, Inria, 9 rue Joliot-Curie, 91190 Gif-sur-Yvette, France
E-mail: hugues.talbot@centralesupelec.fr

1 Introduction

Affine transformations gather a large family of simple, yet important geometric transformations which are useful in various applications of image processing, geometrical modeling or computer graphics. In the Euclidean spaces $\mathbb{R}^n$ ($n \geq 2$), affine transformations are bijective and preserve some important geometrical properties (e.g. parallelism). They also preserve topological properties. This is no longer the case when they are considered in the Cartesian grids $\mathbb{Z}^n$. A simple example of this phenomenon is illustrated in Figure 1.

In Cartesian grids, various subfamilies of affine transformations have been investigated, namely translations [7, 33], scalings [1,3], reflections [5,12], rotations [2,4,5,8,18, 25,44,45,49,54], rigid motions [38,39,41–43,46,50], combined scalings and rotations [22], and affine transformations [11,21,23,24,27,29,37]. The purposes were manifold: describing the combinatorial structure of these transformations with respect to $\mathbb{R}^n$ versus $\mathbb{Z}^n$ [1–3,7,8,18,21–23,33,38,48, 56], guaranteeing their bijectivity [4,5,12,25,44,49,50,54] or their transitivity [45] in $\mathbb{Z}^n$, preserving geometrical properties [41,42] and, less frequently, ensuring their topological invariance [39,43] in $\mathbb{Z}^n$. These are non-trivial questions, and their difficulty increases with the dimension of the Cartesian grid [46]. Indeed, most of these works deal with $\mathbb{Z}^2$ [4,5,7,8,25,33,38–40,42–45,50,54]; fewer with $\mathbb{Z}^3$ [41, 49,56] or $\mathbb{Z}^n$ [18].

Regarding affine transformations, the literature has been dedicated to the so-called quasi-affine (and sometimes quasi-linear) transformations[1]. These transformations were pioneered in [24,37] and studied from a combinatorial point of view, mainly by analyzing the induced tilings of the space in

[1] These quasi-affine transformations are close to the class of affine transformations that we consider in this article. They mainly differ regarding the digitization policy: quasi-affine transformations rely on the floor function, whereas we will consider the rounding function.

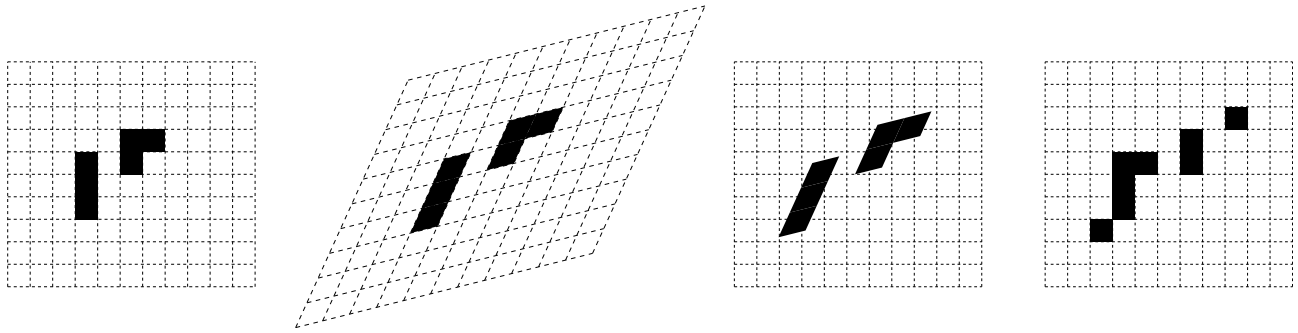

Fig. 1 Example of topological alterations induced by a digital affine transformation. From left to right: input digital image; an affine transformation applied on this image (viewed in a continous way); the same transformed image viewed in the digital grid; the final discretized image, embedded into the digital grid via Gauss digitization. The initial image is composed of two connected components. The final image is composed of 3 (or 4, depending on the considered adjacency) connected components. The topology between both has then been modified.

2 [26], 3 [13] and n dimensions [11,27,29], and by investigating their relations with fractals [28].

In this article, we investigate how it may be possible to preserve the topological properties of a digital object defined in the Cartesian grid when applying an affine transformation.

Previous works related to this topic were geared towards the more restrictive case of rigid motions (i.e. the composition of translations and rotations, but without scalings). In [43] a specific family of digital objects in $\mathbb{Z}^2$, called "regular", was proved to preserve their topology under any rigid motion. However, all the digital objects in $\mathbb{Z}^2$ are not regular, and the required modifications for generating a regular object from a non-regular one induce asymmetric operations between the object and its background. In [39] the putative topology preservation between an object and its image in $\mathbb{Z}^2$ by a rigid motion was checked by searching a path in the combinatorial space of digital rigid motions that corresponds to a point-by-point homotopic transformation between both. However, this process allows to assess the topological invariance, not to ensure it. In addition, both approaches can not easily be extended to the case of affine transformations.

We propose a way of tackling the problem of affine transformations under the constraint of topological invariance. As in [39,43], we consider the case of digital objects in $\mathbb{Z}^2$. Since a digital object X and its usual digital image by an affine transformation $\mathcal{A}$ are not guaranteed to present the same topology, our purpose is to compute a digital object $\widehat{\mathsf{X}}$ that (1) has the same topology as X and (2) is "as similar as possible" to the usual digital image of X by $\mathcal{A}$. In other words, we accept to slightly relax some constraints on geometric similarity in order to ensure topological invariance.

To reach that goal, we embed our digital objects in the Euclidean space and we process them in the (continuous but discrete) space of cellular complexes. This allows us to model / manipulate these objects in a way compliant with both their digital nature and their continuous interpretation (in particular from a topological point of view), but also to carry out basic transformations in a space finer than $\mathbb{Z}^2$. The definition of $\widehat{\mathsf{X}}$ from X and $\mathcal{A}$ is then formulated as an optimization problem, which presents similarities with the topology-preserving paradigms developed in the framework of deformable models [16,17,19,53].

This article is an extended and improved version of the conference paper [47]. The new material is as follows. We extend our approach from rigid to affine transformations. This constitutes a relevant methodological contribution in the field of discrete geometry, where a majority of the proposed topology-preserving geometric transformations are restricted to rotations and rigid transformations and can not be extended to more general affine transformations. We also propose a more complete and fully reproducible description of the modeling part of the approach. In particular, we provide in Appendix A a description of the way of building the cellular space where to carry out the homotopic transformation required by the algorithm. Regarding the optimization part of the process, we provide a gradient descent approach, with a reproducible description, whereas only a sketched description of a general scheme was given in [47]. Finally, we present various experimental results and we compare the behaviour of the proposed transformation approach with other topology-preserving (rigid) transformations schemes that rely on the notions of regularity [43] and quasi-regularity [42], respectively.

The remainder of the article is organized as follows. In Section 2, we introduce the basic notions required to make the article self-contained. In Section 3, we present a summary of the proposed method. Section 4 describes the different cellular spaces required by the method and the way to build and switch between them (this section is completed by Appendix A). Section 5 describes an optimization strategy developed in the space of cellular complexes in order to ensure topology preservation while seeking the result of the affine transformation. Section 6 presents and discusses some results obtained with our method, and compares them

to usual digitization-based transformations. Section 7 provides concluding remarks.

2 Basic Notions

2.1 Affine transformations

We first describe the transformations that we aim to study, namely the affine ones. A point of $\mathbb{R}^2$ (and a fortiori of $\mathbb{Z}^2$) is noted in bold (e.g. $\mathbf{p}$). Its coordinates are noted with subscripts (e.g. $\mathbf{p} = (p_x, p_y)^t$). The transpose symbol is sometimes omitted by abuse of notation (e.g. $\mathbf{p} = (p_x, p_y)$).

An affine tranformation $\mathcal{A} : \mathbb{R}^2 \to \mathbb{R}^2$ is defined, for any point $\mathbf{p} \in \mathbb{R}^2$ as

$$\mathcal{A}(\mathbf{p}) = A \cdot \mathbf{p} + \mathbf{t} = \begin{bmatrix} a_{11} & a_{12} \\ a_{21} & a_{22} \end{bmatrix} \cdot \begin{pmatrix} p_x \\ p_y \end{pmatrix} + \begin{pmatrix} t_x \\ t_y \end{pmatrix} \tag{1}$$

with $A = [a_{i,j}]_{1 \leq i,j \leq 2}$, $\det(A) \neq 0$, and $\mathbf{t} \in \mathbb{R}^2$, where the six parameters $a_{i,j}$ $(1 \leq i, j \leq 2)$ and t_x, t_y are real values.

The affine transformations include, in particular:

- translations ($A = I_2$); and
- when $\mathbf{t} = \mathbf{0}$:
  - rotations ($a_{11} = a_{22} = \cos\theta$, $-a_{12} = a_{21} = \sin\theta$ for $\theta \in \mathbb{R}$);
  - symmetries ($a_{11} = \pm 1, a_{22} = \pm 1, a_{12} = a_{21} = 0$);
  - scalings ($a_{11} \neq 0, a_{22} \neq 0$ and $a_{12} = a_{21} = 0$);

and, of course, all their compositions.

In this work, we assume that the six parameters $a_{i,j}$ $(1 \leq i, j \leq 2)$ and t_x, t_y lie in $\mathbb{Q}$. From an applicative point of view, this is not a restrictive hypothesis. Indeed, translations (resp. scalings) with rational parameters can approximate any translations (resp. scalings) with irrational parameters for any required precision. Regarding the rotations, the parameters a_{11} and a_{21}, that correspond to the cosine and sine of the rotation angle θ can be chosen as $a_{11} = a/c$ and $a_{21} = b/c$, where $(a, b, c) \in \mathbb{Z}^3$ is a Pythagorean triple, i.e. satisfies $a^2 + b^2 = c^2$. This family is sufficiently dense to reasonably handle rotations while manipulating rational values only [6].

We also assume that $\det(A) > 0$. In other words, we only focus on the affine transformations that preserve the orientations, which is a non-restrictive hypothesis in the context of image processing / analysis.

The affine transformation $\mathcal{A}$ of Eq. (1) can then be expressed from $(a_{11}, a_{12}, a_{21}, a_{22}, t_x, t_y) \in \mathbb{Q}^6$. In particular, for any $\mathbf{p} \in \mathbb{Q}^2$, we have

$$\mathcal{A}(\mathbf{p}) = \begin{pmatrix} a_{11}p_x + a_{12}p_y + t_x \\ a_{21}p_x + a_{22}p_y + t_y \end{pmatrix} \in \mathbb{Q}^2 \tag{2}$$

2.2 Cellular complexes

Let $P \subset \mathbb{R}^2$ be a closed, convex polygon. Let $\mathring{P}$ be the interior of P and $\partial P = P \setminus \mathring{P}$ the boundary of P. We note $\mathcal{P}(P) = \{\mathring{P}\}$.

Let $E = [\mathbf{v_1}, \mathbf{v_2}] \subset \partial P$ $(\mathbf{v_1}, \mathbf{v_2} \in \mathbb{R}^2)$ be a maximal, closed line segment of ∂P. Let $\mathring{E} =]\mathbf{v_1}, \mathbf{v_2}[$ be the interior (i.e. the open line segment) of E, and $\partial E = E \setminus \mathring{E}$ be the boundary of E. The open line segment $\mathring{E}$ is called an edge of P. We note $\mathcal{E}(P)$ the set of all the edges of P.

Let $\mathbf{v} \in \partial E$ be a point of ∂E; the singleton set $V = \{\mathbf{v}\}$ is called a vertex of P. We note $\mathcal{V}(P)$ the set of all the vertices of P.

The set

$$\mathcal{F}(P) = \mathcal{P}(P) \cup \mathcal{E}(P) \cup \mathcal{V}(P) \tag{3}$$

is a partition of P.

Let $\Omega \subset \mathbb{R}^2$ be a closed, convex polygon. Let $\mathcal{K}$ be a set of closed, convex polygons such that $\Omega = \bigcup \mathcal{K}$ and for any two distinct polygons $P_1, P_2 \in \mathcal{K}$, we have[2] $\mathring{P}_1 \cap \mathring{P}_2 = \emptyset$. We set[3]

$$\mathbb{K}(\Omega) = \bigcup_{P \in \mathcal{K}} \mathcal{F}(P) \tag{4}$$

It is plain that $\mathbb{K}(\Omega)$ is a partition of Ω. We call $\mathbb{K}(\Omega)$, or simply $\mathbb{K}$, a cellular space (associated to Ω).

Each element $\mathfrak{f}_2$ (resp. $\mathfrak{f}_1$, resp. $\mathfrak{f}_0$) of $\mathbb{K}$ which is the interior (resp. an edge, resp. a vertex) of a polygon $P \in \mathcal{K}$ is called a 2-face (resp. 1-face, resp. 0-face). We set $\mathbb{K}_d$ $(0 \leq d \leq 2, d \in \mathbb{Z})$ the set of all the d-faces of $\mathbb{K}$. More generally, each element of $\mathbb{K}$ is called a face.

Let $\mathfrak{f} \in \mathbb{K}$ be a face. The cell $C(\mathfrak{f})$ induced by $\mathfrak{f}$ is the subset of faces of $\mathbb{K}$ such that $\bigcup C(\mathfrak{f})$ is the smallest closed set that includes $\mathfrak{f}$. If $\mathfrak{f}_0$ is a 0-face, then $C(\mathfrak{f}_0) = \{\mathfrak{f}_0\}$. If $\mathfrak{f}_1$ is a 1-face, then $C(\mathfrak{f}_1) = \{\mathfrak{f}_1, \mathfrak{f}_0^1, \mathfrak{f}_0^2\}$ with $\mathfrak{f}_0^1, \mathfrak{f}_0^2$ the two vertices bounding $\mathfrak{f}_1$, such that $\bigcup C(\mathfrak{f}_1)$ is a closed line segment. If $\mathfrak{f}_2$ is a 2-face, then $C(\mathfrak{f}_2) = \{\mathfrak{f}_2, \mathfrak{f}_1^1, \ldots, \mathfrak{f}_1^k, \mathfrak{f}_0^1, \ldots, \mathfrak{f}_0^k\}$ $(k \geq 3)$ and $\bigcup C(\mathfrak{f}_2)$ is the closed polygon of interior $\mathfrak{f}_2$ with k edges $\mathfrak{f}_1^i$ and k vertices $\mathfrak{f}_0^i$ $(1 \leq i \leq k)$. For any cell $C(\mathfrak{f})$, the face $\mathfrak{f}$ is called the principal face of $C(\mathfrak{f})$, and $C(\mathfrak{f})$ is also called the closure of $\mathfrak{f}$. The star $S(\mathfrak{f})$ of a face $\mathfrak{f}$ is the set of all the faces $\mathfrak{f}'$ such that $\mathfrak{f} \in C(\mathfrak{f}')$.

A face $\mathfrak{f}$ and its induced cell $C(\mathfrak{f})$ are characterized by the list of the 0-faces in $C(\mathfrak{f})$. (In particular we can identify $\mathfrak{f}$ and $C(\mathfrak{f})$ to the sorted (e.g. clockwise) sequence of the k points $\mathbf{v}_i$ $(1 \leq i \leq k)$ that correspond to these 0-faces $\{\mathbf{v}_i\}$.)

[2] If there exist $V_1 = \{\mathbf{v_1}\} \in \mathcal{V}(P_1)$ and $E_2 =]\mathbf{v_2^1}, \mathbf{v_2^2}[\in \mathcal{E}(P_2)$ such that $V_1 \subset E_2$ then, without loss of correctness, we can "modify" the polygon P_2 by adding V_1 into $\mathcal{V}(P_2)$ and by substituting $]\mathbf{v_2^1}, \mathbf{v_1}[$ and $]\mathbf{v_1}, \mathbf{v_2^2}[$ to $]\mathbf{v_2^1}, \mathbf{v_2^2}[$ in $\mathcal{E}(P_2)$.

[3] In theory, this notation will also hold when considering $\mathbb{R}^2$ instead of Ω. In practice, we will always use a bounded subset Ω of $\mathbb{R}^2$.

A complex of $\mathbb{K}$ is a subset $K \subseteq \mathbb{K}$ defined as a union of cells of $\mathbb{K}$. The embedding of K into $\mathbb{R}^2$ is the set noted $\Pi_{\mathbb{R}^2}(K) \subset \mathbb{R}^2$ defined by

$$\Pi_{\mathbb{R}^2}(K) = \bigcup K \tag{5}$$

Let $X \subset \mathbb{R}^2$. If there exists a complex $K \subset \mathbb{K}$ such that $X = \Pi_{\mathbb{R}^2}(K)$, then we say that K is the embedding of X into $\mathbb{K}$ and we note $K = \Pi_{\mathbb{K}}(X)$.

Let $\mathbb{K}$ and $\mathbb{J}$ be two cellular spaces, and $K \subseteq \mathbb{K}$, $J \subseteq \mathbb{J}$ be two complexes. If we have $\Pi_{\mathbb{R}^2}(K) = \Pi_{\mathbb{R}^2}(J)$, i.e. if both complexes correspond to the same continuous object, we note $K \equiv \Pi_{\mathbb{K}}(J)$ and $J \equiv \Pi_{\mathbb{J}}(K)$.

In this work, we will only consider complexes composed as unions of cells with principal 2-faces. The set of all the complexes that can be defined that way on a cellular space $\mathbb{K}$ is noted $\mathbf{C}_{\mathbb{K}}$.

2.3 Topological models and homotopic transformations

Our inputs and outputs are digital objects, namely finite subsets of $\mathbb{Z}^n$ (here with $n = 2$). The topological structure of such objects can be modeled in the framework of digital topology [52]. In this framework, the topological structure of X and its complement $\overline{\mathsf{X}} = \mathbb{Z}^n \setminus \mathsf{X}$ is represented by adjacency relations [51]. More precisely, X is structured with respect to the (3^n-1)- (resp. $2n$-) adjacency, while $\overline{\mathsf{X}}$ is considered with the dual $2n$- (resp. (3^n-1)-) adjacency, in order to avoid topological paradoxes related to the Jordan theorem. In practice, two points $\mathbf{x}$ and $\mathbf{y}$ of $\mathbb{Z}^n$ are $2n$- (resp. (3^n-1)-) adjacent if

$$\|\mathbf{x} - \mathbf{y}\|_p = 1 \tag{6}$$

for $p = 1$ (resp. $p = \infty$). Without loss of generality, we consider X with the (3^n-1)-adjacency (otherwise, it is sufficient to consider $\overline{\mathsf{X}}$ instead of X as the object).

During the methodological process described hereafter, the handled digital objects will be modeled as their continuous analogue, i.e. as closed subsets of $\mathbb{R}^n$ (in particular when carrying out the affine transformations) but also as discrete structures, namely complexes on a given cellular space $\mathbb{K}$ (in particular when carrying out homotopic transformations).

It is possible to deal with this digital–continuous analogy between the objects of $\mathbb{Z}^n$ and those of $\mathbb{R}^n$, via the (intermediate) framework of cellular complexes, formalized in [31] in the case of cubical complexes. Indeed, the three associated topological models are compliant [34,36]. It is also important to note that the cubical cellular spaces can be refined into non-regular cellular spaces (see e.g. [10]), such as defined in Section 2.2 without losing their topological compliance.

The objects that we manipulate must preserve their topological properties. To satisfy this constraint, we consider a strong topological invariant, namely the homotopy type. This choice is relevant for two reasons. On the one hand, in dimension 2, the homotopy type is equivalent to most of the other usual topological invariants. On the other hand, there exist efficient topological tools that allow one to modify an object while preserving its homotopy type.

Given two objects X and Y in $\mathbb{Z}^n$, we prove that they have the same homotopy type by explicitly building a homotopic transformation from X to Y. In the field of digital topology, this is generally done by considering the notion of simple point. In $\mathbb{Z}^n$, a point $\mathbf{x} \in \mathsf{X}$ (resp. $\mathbf{x} \notin \mathsf{X}$) is simple if its removal (resp. addition) from (resp. to) X rewrites as a (monotonic) homotopic transformation. In the framework of digital topology, simple points can be characterized by local, combinatorial properties until $\mathbb{Z}^3$ [9,55].

This notion of simple point, initially defined in digital topology, can be expressed in the framework of cubical complexes, leading to an analogue notion of simple cell [14]. It can also be extended without difficulty to any cellular complex, thanks to the atomic notion of collapse [57].

In this work, the notion of simpleness is considered only in the cellular spaces and in dimension 2 (Section 2.2). Under these hypotheses, the notion of simple cell can be characterized as follows. Let K be a complex defined on a cellular space $\mathbb{K}$ on $\mathbb{R}^2$. Let $\mathfrak{f}_2$ be a 2-face of K. Let $D_0(\mathfrak{f}_2)$ (resp. $D_1(\mathfrak{f}_2)$) be the subset of $C(\mathfrak{f}_2)$ composed by the 0- (resp. 1-) faces $\mathfrak{f}$ the star of which intersects K only within $C(\mathfrak{f}_2)$, i.e. $S(\mathfrak{f}) \cap K = S(\mathfrak{f}) \cap C(\mathfrak{f}_2)$. We say that $C(\mathfrak{f}_2)$ is a simple cell (for K) iff[4]

$$|\, D_1(\mathfrak{f}_2)\,| = |\, D_0(\mathfrak{f}_2)\,| + 1 \tag{7}$$

with $|\cdot|$ the cardinal on finite sets. In such case, the detachment of this 2-cell $C(\mathfrak{f}_2)$ from K, i.e. the operation that transforms K into

$$K \oslash C(\mathfrak{f}_2) = K \setminus (\{\mathfrak{f}_2\} \cup D_1(\mathfrak{f}_2) \cup D_0(\mathfrak{f}_2)) \tag{8}$$

corresponds to a collapse operation from K to $K \oslash C(\mathfrak{f}_2)$, and both complexes have the same homotopy type. Reversely, if $\mathfrak{f}_2$ is a 2-face of $\mathbb{K} \setminus K$, and if $C(\mathfrak{f}_2)$ is a simple 2-cell for the complex $K \cup C(\mathfrak{f}_2)$, then the operation of attachment that transforms K into $K \cup C(\mathfrak{f}_2)$ corresponds to the reverse collapse operation from $K \cup C(\mathfrak{f}_2)$ into K, and both complexes also have the same homotopy type.

For the sake of concision, in the sequel, we will note

$$K \circledcirc C(\mathfrak{f}_2) = \begin{cases} K \oslash C(\mathfrak{f}_2) & \text{if } \mathfrak{f}_2 \in K \\ K \cup C(\mathfrak{f}_2) & \text{if } \mathfrak{f}_2 \notin K \end{cases} \tag{9}$$

This notation holds independently from the simpleness or non-simpleness of $C(\mathfrak{f}_2)$.

[4] This is equivalent to say that the intersection of the border of $C(\mathfrak{f}_2)$ (i.e. $C(\mathfrak{f}_2) \setminus \{\mathfrak{f}_2\}$) and $K \oslash C(\mathfrak{f}_2)$ (see Eq. (8)) has a Euler characteristics of 1 (and is then also non-empty and connected), which is a necessary and sufficient condition for simpleness in dimension 2.

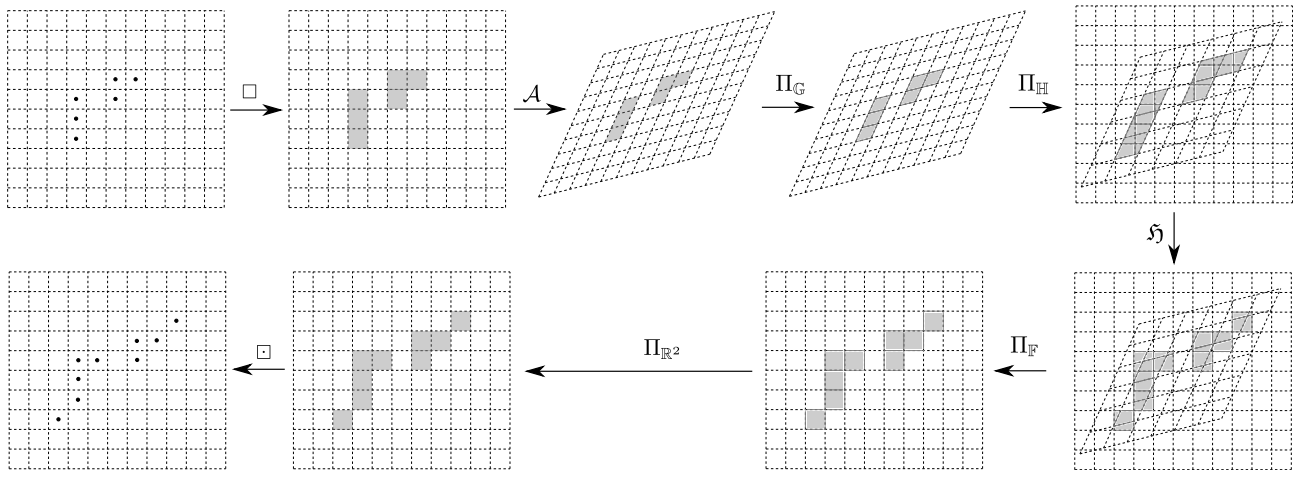

Fig. 2 Proposed framework for homotopy type preserving affine transformation. Following the flowchart (see Section 3.3): $\mathsf{X} \subset \mathbb{Z}^2$; (1) $\square\mathsf{X} = X \subset \mathbb{R}^2$; (2) $\mathcal{A}(X) = X_{\mathcal{A}} \subset \mathbb{R}^2$; (3) $\Pi_{\mathbb{G}}(X_{\mathcal{A}}) = G \in \mathbf{C}_{\mathbb{G}}$, (4) $\Pi_{\mathbb{H}}(G) \equiv H \in \mathbf{C}_{\mathbb{H}}$; (5) $\mathfrak{H}(H) = \widehat{H} \in \mathbf{C}_{\mathbb{H}}$, (6) $\Pi_{\mathbb{F}}(\widehat{H}) \equiv \widehat{F} \in \mathbf{C}_{\mathbb{F}}$; (7) $\Pi_{\mathbb{R}^2}(\widehat{F}) = \widehat{X} \subset \mathbb{R}^2$; (8) $\boxdot\widehat{X} = \widehat{\mathsf{X}} \subset \mathbb{Z}^2$.

3 Overview of the Method

3.1 Problem statement

Given a digital object $\mathsf{X} \subset \mathbb{Z}^2$ and an affine transformation $\mathcal{A} : \mathbb{R}^2 \to \mathbb{R}^2$, we aim to define a digital object $\widehat{\mathsf{X}} \subset \mathbb{Z}^2$ resulting from the application of $\mathcal{A}$ on X.

Of course the direct application of $\mathcal{A}$ on X is generally not an appropriate solution, since in most cases, we have $\mathbf{x} \in \mathbb{Z}^2 \nRightarrow \mathcal{A}(\mathbf{x}) \in \mathbb{Z}^2$. Then, we search a solution $\widehat{\mathsf{X}} \subset \mathbb{Z}^2$ that is "as close as possible" (but generally not equal) to $\mathcal{A}(\mathsf{X}) \subset \mathbb{R}^2$.

Since affine transformations are topologically preserving in $\mathbb{R}^2$, we also require that the sought solution $\widehat{\mathsf{X}} \subset \mathbb{Z}^2$ has the same topology as the initial object $\mathsf{X} \subset \mathbb{Z}^2$.

To summarize, we aim at building a digital object $\widehat{\mathsf{X}}$ that:

- preserves exactly the topology of X; and
- preserves as much as possible the geometry of X;

with respect to the affine transformation $\mathcal{A}$.

3.2 Input and output

The proposed method has the following inputs:

- a (finite) digital object $\mathsf{X} \subset \mathbb{Z}^2$;
- a (rational) affine transformation $\mathcal{A} : \mathbb{Q}^2 \to \mathbb{Q}^2$ (Eq. (1));

and as hyper-parameter:

- a geometric measure $\mathcal{D}^\star : 2^{\mathbb{Z}^2} \times 2^{\mathbb{Z}^2} \to \mathbb{R}_+$ used for determining the geometric (dis)similarity between two digital objects (with respect to $\mathcal{A}$).

The method provides as output:

- a (finite) digital object $\widehat{\mathsf{X}} \subset \mathbb{Z}^2$

such that:

- $\widehat{\mathsf{X}}$ is as close as possible to the image of X by $\mathcal{A}$, which is expressed by minimizing the measure $\mathcal{D}^\star$ between $\widehat{\mathsf{X}}$ and X;
- X and $\widehat{\mathsf{X}}$ have the same homotopy type.

3.3 Main steps of the method

The proposed method, illustrated in Figure 2, can be decomposed into 8 successive steps.

(1) Embedding in $\mathbb{R}^2$
We define $X \subset \mathbb{R}^2$, the continuous analogue of X, as

$$X = \mathsf{X} \oplus \square \tag{10}$$

where $\oplus$ is the usual dilation operator [20] and $\square$ is the closed, unit square structuring element $[-\frac{1}{2}, \frac{1}{2}]^2 \subset \mathbb{R}^2$. In other words, X is the union of pixels centered at the points of X. We note

$$\left| \begin{array}{l} \square : 2^{\mathbb{Z}^2} \to 2^{\mathbb{R}^2} \\ \quad \mathsf{X} \quad \mapsto \square(\mathsf{X}) = \mathsf{X} \oplus \square = X \end{array} \right. \tag{11}$$

the function that defines this continuous analogue. For the sake of concision, we will sometimes note $\square\mathsf{X}$ instead of $\square(\mathsf{X})$.

(2) Affine transformation in $\mathbb{R}^2$
The affine transformation $\mathcal{A}$ is applied on the continuous object X (Eq. (1)), leading to the continuous object

$$X_{\mathcal{A}} = \mathcal{A}(X) = \{\mathcal{A}(\mathbf{x}) \mid \mathbf{x} \in X\} \subset \mathbb{R}^2 \tag{12}$$

(3) Embedding in the cellular space $\mathbb{G}$
The continuous object $X_{\mathcal{A}}$ is embedded in a cellular space

$\mathbb{G}$ which is the image by $\mathcal{A}$ of the canonical cubical space $\mathbb{F}$ induced by $\mathbb{Z}^2$. We note

$$G = \Pi_{\mathbb{G}}(X_{\mathcal{A}}) \tag{13}$$

the complex induced by the embedding of $X_{\mathcal{A}}$ in $\mathbb{G}$. The definition of both cellular spaces $\mathbb{F}$ and $\mathbb{G}$ and the way to compute $\Pi_{\mathbb{G}}(X_{\mathcal{A}})$ are detailed in Sections 4.1 and 4.2.

(4) Embedding in the cellular space $\mathbb{H}$
In the next steps of the method, our purpose is to build a homotopic transformation for turning the complex G into another complex $\widehat{F}$ that will be finally embedded back into $\mathbb{Z}^2$. This requires that $\widehat{F}$ be defined in the cubical space $\mathbb{F}$ whereas G is defined in the cellular space $\mathbb{G}$. To tackle this issue, we define a cellular space $\mathbb{H}$ that refines both $\mathbb{F}$ and $\mathbb{G}$, and we embed G into $\mathbb{H}$. We note

$$H \equiv \Pi_{\mathbb{H}}(G) = \Pi_{\mathbb{H}}(X_{\mathcal{A}}) \tag{14}$$

the complex obtained by refining the complex G into the cellular space $\mathbb{H}$. The definition of the cellular space $\mathbb{H}$ and the way to compute H are detailed in Section 4.3.

(5) Construction of an optimal complex in $\mathbb{H}$
At this stage, we aim to define a complex $\widehat{H}$ that satisfies the required properties with respect to our problem. First, $\widehat{H}$ has to be obtained from H (which has the same homotopy type as X) via a homotopic transformation $\mathfrak{H}$ in the cubical space $\mathbb{H}$. Second, $\widehat{H}$ must be embeddable into the coarser cubical space $\mathbb{F}$, i.e. there must exist a cubical complex $\widehat{F}$ in $\mathbb{F}$ such that

$$\widehat{F} \equiv \Pi_{\mathbb{F}}(\widehat{H}) \tag{15}$$

Third, the digital object $\widehat{\mathsf{X}}$ that will be derived from (and will have the same homotopy type as) $\widehat{H}$ and $\widehat{F}$ should be "as similar as possible" to the digital object X given as input, with respect to the affine transformation $\mathcal{A}$. This is expressed by the fact that we aim at reaching

$$\min \mathcal{D}^{\star}(\mathsf{X}, \widehat{\mathsf{X}}) \tag{16}$$

for the chosen measure $\mathcal{D}^{\star}$. The handling of this constrained optimization process is described in Section 5.

(6) Embedding in the cellular space $\mathbb{F}$
For the further digitization purpose, it is mandatory that $\widehat{H}$ be rewritten as a complex $\widehat{F}$ defined in the cubical space $\mathbb{F}$. This is tractable from Eq. (15). The way to pass from $\mathbb{H}$ to $\mathbb{F}$ is detailed in Section 4.3.

(7) Embedding in $\mathbb{R}^2$
The complex $\widehat{F}$ is embedded into $\mathbb{R}^2$ by following the formulation of Eq. (5), i.e.

$$\widehat{X} = \Pi_{\mathbb{R}^2}(\widehat{F}) = \bigcup \widehat{F} \tag{17}$$

(8) Embedding in $\mathbb{Z}^2$
The continuous object $\widehat{X}$ is embedded into $\mathbb{Z}^2$ by following the usual Gauss digitization paradigm [30]

$$\widehat{\mathsf{X}} = \widehat{X} \cap \mathbb{Z}^2 \tag{18}$$

The function that defines the Gauss digitization[5] of a continuous object is noted

$$\left| \begin{array}{rcl} \boxdot : 2^{\mathbb{R}^2} & \to & 2^{\mathbb{Z}^2} \\ Y & \mapsto & \boxdot(Y) = Y \cap \mathbb{Z}^2 \end{array} \right. \tag{19}$$

For the sake of concision, we will sometimes note $\boxdot Y$ instead of $\boxdot(Y)$. We then have $\widehat{\mathsf{X}} = \boxdot \widehat{X}$.

Summary
Overall, we then define $\widehat{\mathsf{X}}$ from X as

$$\widehat{\mathsf{X}} = \big[\underbrace{\boxdot \circ \Pi_{\mathbb{R}^2} \circ \Pi_{\mathbb{F}}}_{(6\text{–}8)} \circ \mathfrak{H} \circ \underbrace{\Pi_{\mathbb{H}} \circ \Pi_{\mathbb{G}} \circ \mathcal{A} \circ \square}_{(1\text{–}4)} \big] (\mathsf{X}) \tag{20}$$

where the two parts corresponding to steps (1–4) and (6–8) are related to geometric and structural operations (that preserve the homotopy type), while step 5, namely the construction of the homotopic transformation $\mathfrak{H}$ corresponds to the optimization part of the process.

4 Cellular Complexes

4.1 The initial cubical space $\mathbb{F}$

The initial digital object X is defined in $\mathbb{Z}^2$, and so is the final digital object $\widehat{\mathsf{X}}$ that we aim to build. Both have a continuous analogue in $\mathbb{R}^2$. The continuous analogue X of X is defined as $X = \square\mathsf{X}$. The continuous analogue $\widehat{X}$ of $\widehat{\mathsf{X}}$ is characterized by $\widehat{X} = \square\widehat{\mathsf{X}}$. In other words, both are defined as unions of unit, closed squares (i.e. pixels) centered on the points of X and $\widehat{\mathsf{X}}$, respectively. In order to model / manipulate these two continuous objects X and $\widehat{X}$ of $\mathbb{R}^2$ as complexes, we build the cellular (actually cubical) complex space $\mathbb{F}$ as follows.

Let us set

$$\Delta = \mathbb{Z} + \frac{1}{2} = \left\{ k + \frac{1}{2} \mid k \in \mathbb{Z} \right\} \tag{21}$$

Let $\delta \in \Delta$. We define the vertical line $V_\delta \subset \mathbb{R}^2$ and the horizon line $H_\delta \subset \mathbb{R}^2$ by the following equations, respectively

$$(V_\delta) \quad x - \delta = 0 \tag{22}$$

$$(H_\delta) \quad y - \delta = 0 \tag{23}$$

[5] The choice of Gauss digitization is relevant with respect to Step (1) since we have $\boxdot\square = Id_{2^{\mathbb{Z}^2}}$.

We set

$$\mathcal{V}_\Delta = \{V_\delta \mid \delta \in \Delta\} \tag{24}$$
$$\mathcal{H}_\Delta = \{H_\delta \mid \delta \in \Delta\} \tag{25}$$
$$\mathcal{G}_\Delta = \mathcal{V}_\Delta \cup \mathcal{H}_\Delta \tag{26}$$

This last set $\mathcal{G}_\Delta$ is the square grid that subdivides $\mathbb{R}^2$ into unit squares centered on the points of $\mathbb{Z}^2$. In other words, $\mathcal{G}_\Delta$ generates the Voronoi diagram of $\mathbb{Z}^2$ in $\mathbb{R}^2$.

The induced cellular complex space $\mathbb{F}(\mathbb{R}^2)$, simply noted $\mathbb{F}$, is then composed of the sets $\mathbb{F}_0$, $\mathbb{F}_1$ and $\mathbb{F}_2$ of 0-, 1- and 2-faces defined as

$$\mathbb{F}_0 = \{\{\mathbf{d}\} \mid \mathbf{d} \in \Delta^2\} \tag{27}$$
$$\mathbb{F}_1 = \{]\mathbf{d}, \mathbf{d} + \mathbf{e}_x[\mid \mathbf{d} \in \Delta^2\} \cup \{]\mathbf{d}, \mathbf{d} + \mathbf{e}_y[\mid \mathbf{d} \in \Delta^2\} \tag{28}$$
$$\mathbb{F}_2 = \{]\mathbf{d}, \mathbf{d} + \mathbf{e}_x[\times]\mathbf{d}, \mathbf{d} + \mathbf{e}_y[\mid \mathbf{d} \in \Delta^2\} \tag{29}$$

where $\mathbf{e}_x = (1, 0)$ and $\mathbf{e}_y = (0, 1)$. In particular, we have

$$\bigcup \mathbb{F}_0 = \mathcal{V}_\Delta \cap \mathcal{H}_\Delta \tag{30}$$
$$\bigcup \mathbb{F}_1 = \mathcal{G}_\Delta \setminus (\mathcal{V}_\Delta \cap \mathcal{H}_\Delta) \tag{31}$$
$$\bigcup \mathbb{F}_2 = \mathbb{R}^2 \setminus \mathcal{G}_\Delta \tag{32}$$

For a digital object $\mathsf{X} \subset \mathbb{Z}^2$ and its continuous analogue $X = \square\mathsf{X}$, we define the associated complex $F = \Pi_{\mathbb{F}}(X) \in \mathbf{C}_{\mathbb{F}}$ as

$$F = \bigcup_{\mathbf{x} \in \mathsf{X}} C(\blacksquare\mathbf{x}) = \{\mathfrak{f} \in \mathbb{F} \mid \mathfrak{f} \subset X\} \tag{33}$$

where

$$\left| \begin{array}{l} \blacksquare : \mathbb{Z}^2 \to \mathbb{F}_2 \\ \quad \mathbf{p} \ \mapsto \mathbf{p} \oplus]-\frac{1}{2}, \frac{1}{2}[^2 \end{array} \right. \tag{34}$$

is the bijective function that maps each $\mathbf{p} \in \mathbb{Z}^2$ to its associated unit, open square (i.e. 2-face) $\blacksquare(\mathbf{p})$, also noted $\blacksquare\mathbf{p}$.

We set $\mathbb{F}_d(F)$ $(0 \leq d \leq 2)$ the set of all the d-faces of F. In particular, we have

$$X = \square\mathsf{X} = \bigcup \Pi_{\mathbb{F}}(X) = \Pi_{\mathbb{R}^2}(F) \tag{35}$$
$$\mathsf{X} = \boxdot X = \blacksquare^{-1}(\mathbb{F}_2(F)) \tag{36}$$

4.2 The cellular space $\mathbb{G}$ induced by $\mathcal{A}$

The affine transformation $\mathcal{A}$ is applied on the continuous analogue $X \subset \mathbb{R}^2$ of X, leading to the continuous object $\mathcal{A}(X) = X_{\mathcal{A}} \subset \mathbb{R}^2$ (see Eq. (12)).

Similarly to X, that can be modeled by a complex F in the cubical space $\mathbb{F}$ (Section 4.1), the object $X_{\mathcal{A}}$ can also be modeled by a complex G in a cellular space $\mathbb{G}$. This cellular space $\mathbb{G}$ is the image of $\mathbb{F}$ by the affine transformation $\mathcal{A}$. In particular, $\mathcal{A}$ trivially induces an isomorphism between these two spaces.

More precisely, $\mathbb{G}$ derives from the grid $\mathcal{A}(\mathcal{G}_\Delta)$ which subdivides $\mathbb{R}^2$ into parallelograms centered on the points of $\mathcal{A}(\mathbb{Z}^2)$. We have

$$\mathcal{A}(\mathcal{G}_\Delta) = \mathcal{A}(\mathcal{V}_\Delta) \cup \mathcal{A}(\mathcal{H}_\Delta) \tag{37}$$

with

$$\mathcal{A}(\mathcal{V}_\Delta) = \{\mathcal{A}(V_\delta) \mid \delta \in \Delta\} \tag{38}$$
$$\mathcal{A}(\mathcal{H}_\Delta) = \{\mathcal{A}(H_\delta) \mid \delta \in \Delta\} \tag{39}$$

For each $\delta \in \Delta$, the lines $\mathcal{A}(V_\delta)$ and $\mathcal{A}(H_\delta)$ are defined by the following equations, respectively

$$(\mathcal{A}(V_\delta)) \qquad a_{22}x - a_{12}y - a_{22}t_x + a_{12}t_y - \delta = 0 \tag{40}$$
$$(\mathcal{A}(H_\delta)) \qquad -a_{21}x + a_{11}y + a_{21}t_x - a_{11}t_y - \delta = 0 \tag{41}$$

The induced cellular space $\mathbb{G}$ is then composed of the three sets of d-faces $(0 \leq d \leq 2)$

$$\mathbb{G}_d = \mathcal{A}(\mathbb{F}_d) = \{\mathcal{A}(\mathfrak{f}) \mid \mathfrak{f} \in \mathbb{F}_d\} \tag{42}$$

The continuous object $X_{\mathcal{A}} \subset \mathbb{R}^2$ is then modeled by the complex $G = \Pi_{\mathbb{G}}(X_{\mathcal{A}}) \in \mathbf{C}_{\mathbb{G}}$

$$G = \mathcal{A}(F) = \mathcal{A}(\Pi_{\mathbb{F}}(X)) = \{\mathcal{A}(\mathfrak{f}) \mid \mathfrak{f} \in \Pi_{\mathbb{F}}(X)\} \tag{43}$$

We set $\mathbb{G}_d(G)$ $(0 \leq d \leq 2)$ the set of all the d-faces of G.

4.3 The cellular space $\mathbb{H}$ refining the spaces $\mathbb{F}$ and $\mathbb{G}$

Although $X_{\mathcal{A}}$ presents good topological properties with respect to X, it cannot be directly used for building the final digital object $\widehat{\mathsf{X}}$. Indeed, the complex G that models $X_{\mathcal{A}}$ is defined on $\mathbb{G}$ and not on $\mathbb{F}$.

At this stage, our purpose is to build from the complex G in $\mathbb{G}$, a new (cubical) complex $\widehat{F}$ in $\mathbb{F}$, that will be used to finally define the resulting digital object $\widehat{\mathsf{X}}$. In order to guarantee the preservation of the homotopy type between X and $\widehat{\mathsf{X}}$, it is indeed necessary that G and $\widehat{F}$ also have the same homotopy type, i.e. we have to build $\widehat{F}$ from G via a homotopic transformation. This requires that both of these complexes be defined in the same cellular space.

Then, we build a new cellular space $\mathbb{H}$ that refines both $\mathbb{F}$ and $\mathbb{G}$. In this space $\mathbb{H}$, the 2-faces are convex polygons of various shapes (whereas they are only squares and parallelograms in $\mathbb{F}$ and $\mathbb{G}$, respectively).

Practically, $\mathbb{H}$ is built from the subdivision of the Euclidean plane $\mathbb{R}^2$ by the union of the two grids $\mathcal{G}_\Delta$ and $\mathcal{A}(\mathcal{G}_\Delta)$. In particular, for each 2-face $\mathfrak{h}_2$ of $\mathbb{H}$, there exists exactly one 2-face $\mathfrak{f}_2$ of $\mathbb{F}$ and one 2-face $\mathfrak{g}_2$ of $\mathbb{G}$ such that

$$\mathfrak{h}_2 = \mathfrak{f}_2 \cap \mathfrak{g}_2 \tag{44}$$

Based on this property, we define the two functions $\phi : \mathbb{H}_2 \to \mathbb{F}_2$ and $\gamma : \mathbb{H}_2 \to \mathbb{G}_2$, such that

$$\phi(\mathfrak{h}_2) = \mathfrak{f}_2 \tag{45}$$

$$\gamma(\mathfrak{h}_2) = \mathfrak{g}_2 \tag{46}$$

Reversely, we build the two functions

$$\left| \begin{array}{l} \Phi : \mathbb{F}_2 \to 2^{\mathbb{H}_2} \\ \quad \mathfrak{f}_2 \ \mapsto \phi^{-1}(\{\mathfrak{f}_2\}) = \{\mathfrak{h}_2 \in \mathbb{H}_2 \mid \phi(\mathfrak{h}_2) = \mathfrak{f}_2\} \end{array} \right. \tag{47}$$

and

$$\left| \begin{array}{l} \Gamma : \mathbb{G}_2 \to 2^{\mathbb{H}_2} \\ \quad \mathfrak{g}_2 \ \mapsto \gamma^{-1}(\{\mathfrak{g}_2\}) = \{\mathfrak{h}_2 \in \mathbb{H}_2 \mid \gamma(\mathfrak{h}_2) = \mathfrak{g}_2\} \end{array} \right. \tag{48}$$

The algorithmic process for building $\mathbb{H}$ from $\mathbb{F}$ and $\mathbb{G}$ is detailed in Appendix A. This process can be carried out using only exact calculus since all the 0-faces of $\mathbb{H}$ have rational coordinates. Indeed, from Eqs. (22–23) and (40–41), the lines of $\mathscr{G}_\Delta$ and $\mathcal{A}(\mathscr{G}_\Delta)$ have rational-coefficient equations. In particular, for two (non-colinear) such lines L_i ($1 \leq i \leq 2$) of equations

$$a_i x + b_i y + c_i = 0 \tag{49}$$

with $a_i, b_i, c_i \in \mathbb{Q}$, the putative point of intersection $\mathbf{d}$ between both forming a 0-face $\{\mathbf{d}\}$ of $\mathbb{H}$ has the following coordinates:

$$(d_x, d_y) = \left(\frac{b_1 c_2 - b_2 c_1}{a_1 b_2 - a_2 b_1}, \frac{a_1 c_2 - a_2 c_1}{a_2 b_1 - a_1 b_2} \right) \in \mathbb{Q}^2 \tag{50}$$

It is important that the data structure finally modeling $\mathbb{H}$ allows us to have access easily to $C(\mathfrak{h})$, $S(\mathfrak{h})$ for any face $\mathfrak{h}$ of $\mathbb{H}$, but also to have access to $\phi(\mathfrak{h}_2)$ and $\gamma(\mathfrak{h}_2)$ for any 2-face $\mathfrak{h}_2$ of $\mathbb{H}$ and to $\Phi(\mathfrak{f}_2)$ and $\Gamma(\mathfrak{g}_2)$ for any 2-faces $\mathfrak{f}_2$ of $\mathbb{F}$ and $\mathfrak{g}_2$ of $\mathbb{G}$.

Based on the above functions, each complexes F on $\mathbb{F}$ and G of $\mathbb{G}$ can be embedded into $\mathbb{H}$ by defining the complex $\Pi_{\mathbb{H}}(F)$ and $\Pi_{\mathbb{H}}(G)$, respectively, as

$$\Pi_{\mathbb{H}}(F) = \bigcup_{\mathfrak{f}_2 \in \mathbb{F}_2(F)} \bigcup_{\mathfrak{h}_2 \in \Phi(\mathfrak{f}_2)} C(\mathfrak{h}_2) \tag{51}$$

$$\Pi_{\mathbb{H}}(G) = \bigcup_{\mathfrak{g}_2 \in \mathbb{G}_2(G)} \bigcup_{\mathfrak{h}_2 \in \Gamma(\mathfrak{g}_2)} C(\mathfrak{h}_2) \tag{52}$$

For any complex H on $\mathbb{H}$, if there exists a complex F on $\mathbb{F}$ (resp. G on $\mathbb{G}$) such that $H \equiv \Pi_{\mathbb{H}}(F)$ (resp. $H \equiv \Pi_{\mathbb{H}}(G)$), then we have

$$F = \Pi_{\mathbb{F}}(H) = \bigcup_{\mathfrak{h}_2 \in \mathbb{H}_2(H)} C(\phi(\mathfrak{h}_2)) \tag{53}$$

$$G = \Pi_{\mathbb{G}}(H) = \bigcup_{\mathfrak{h}_2 \in \mathbb{H}_2(H)} C(\gamma(\mathfrak{h}_2)) \tag{54}$$

5 Optimization-Based Affine Transformation

In this section, we discuss on the optimization part of the proposed method. It corresponds to the computation of the homotopic transformation $\mathfrak{H}$ between the complexes H and $\widehat{H}$ in the cellular space $\mathbb{H}$, i.e. Step (5) in Section 3.3.

The sought complex $\widehat{H}$ has to satisfy three properties:

1. it must have the same homotopy type as H;
2. it must be embeddable into the coarser cubical space $\mathbb{F}$;
3. it must allow to minimize the measure $\mathcal{D}^\star$ (Eq. (16)) with respect to the object X and the affine transformation $\mathcal{A}$.

Hereatfer, we express more formally these three properties.

5.1 Objective functions

We recall that the complex H corresponds to the exact embedding of the digital image X in the cellular space $\mathbb{H}$. More precisely, we have

$$H = \left[\Pi_{\mathbb{H}} \circ \Pi_{\mathbb{G}} \circ \mathcal{A} \circ \square \right](\mathsf{X}) \tag{55}$$

which corresponds to the "(1–4)" part of Eq. (20). In particular, the digital object $\mathsf{X} \subset \mathbb{Z}^2$ is expressed as a continous object X of $\mathbb{R}^2$, then it undergoes an affine transformation, and is embedded first into the cellular space $\mathbb{G}$ and second into the finer cellular space $\mathbb{H}$.

Let us consider a complex $\widetilde{H}$ of the cellular space $\mathbb{H}$. We explain how H and $\widetilde{H}$ may differ with respect to the three above properties.

5.1.1 Topological error measure

In dimension 2, it is possible to accurately quantify the topological difference between the two complexes H and $\widetilde{H}$, i.e. to define a topological error measure $\mathcal{E}_{\text{topo}} : \mathbf{C}_{\mathbb{H}} \times \mathbf{C}_{\mathbb{H}} \to \mathbb{R}_+$. In our case, the purpose is to ensure the preservation of the topology between H and $\widetilde{H}$. Thus, we will simply impose that $\mathcal{E}_{\text{topo}}(H, \widetilde{H}) = 0$, i.e. that H and $\widetilde{H}$ have the same topology. More precisely, we will ensure this property in the algorithmic process by explicitly building a homotopy between these two complexes.

5.1.2 Digitization error measure

The cellular space $\mathbb{H}$ refines the cellular (cubical) space $\mathbb{F}$. In particular, any complex of $\mathbf{C}_{\mathbb{F}}$ corresponds to an analogue complex of $\mathbf{C}_{\mathbb{H}}$. However, the counterpart is not true, in general: only a subset of complexes of $\mathbf{C}_{\mathbb{H}}$ have an analogue complex in $\mathbf{C}_{\mathbb{F}}$. More precisely, the complex $\widetilde{H}$ admits such analogue $\widetilde{F}$ iff for any 2-face $\mathfrak{h}_2$ of $\mathbb{H}$, we have

$$\Phi(\phi(\mathfrak{h}_2)) \cap \widetilde{H} = \Phi(\phi(\mathfrak{h}_2)) \text{ or } \emptyset \tag{56}$$

or equivalently, if for any 2-face $\mathfrak{f}_2$ of $\mathbb{F}$, we have

$$\Phi(\mathfrak{f}_2) \cap \widetilde{H} = \Phi(\mathfrak{f}_2) \text{ or } \emptyset \tag{57}$$

Less formally, this means that any 2-face of $\mathbb{F}$ may be fully embedded either in $\widetilde{H}$ or in its complement (i.e. its background), or equivalently, that it is not "composed" of both complex and background parts.

Based on these facts, it is possible to define a digitization error measure $\mathcal{E}_{\text{digi}} : \mathbf{C}_{\mathbb{H}} \to \mathbb{R}_+$. This can be done, for instance, by computing the number or the area of the 2-faces of $\mathbb{H}$ that forbid to satisfy the property expressed by Eqs. (56–57).

In particular, we have $\mathcal{E}_{\text{digi}}(\widetilde{H}) = 0$ iff there exists $\widetilde{F}$ in $\mathbf{C}_{\mathbb{F}}$ such that $\widetilde{F} \equiv \Pi_{\mathbb{F}}(\widetilde{H})$.

5.1.3 Geometric error measure

We are seeking a digital object $\widehat{\mathsf{X}} \subset \mathbb{Z}^2$ which is as similar as possible to the initial digital object $\mathsf{X} \subset \mathbb{Z}^2$ up to the affine transformation $\mathcal{A}$. This geometrical similarity between these two digital objects X (that underwent $\mathcal{A}$) and $\widehat{\mathsf{X}}$ depends on the similarity between their continuous analogues $X_{\mathcal{A}}$ and $\widehat{X}$ in $\mathbb{R}^2$ (and equivalently between the associated complexes H and $\widehat{H}$ in the cellular space $\mathbb{H}$) but also on the chosen digitization policy that links these continuous and digital objects.

In particular, two main digitization models are frequently considered in the literature, namely the Gauss digitization and the majority vote model. In the Gauss digitization model, our purpose is that $\widehat{\mathsf{X}}$ be as similar as possible to $\boxdot X_{\mathcal{A}}$. In the majority vote model, our purpose is that $\square\widehat{\mathsf{X}}$ be as similar as possible to $X_{\mathcal{A}}$. These two strategies lead to the following measures on digital objects, respectively

$$\mathcal{D}^{\boxdot}(\mathsf{X}, \widehat{\mathsf{X}}) = |\, \boxdot\, \mathcal{A}(\square\mathsf{X}) \otimes \widehat{\mathsf{X}}\,| \tag{58}$$

$$\mathcal{D}^{\square}(\mathsf{X}, \widehat{\mathsf{X}}) = |\, \mathcal{A}(\square\mathsf{X}) \otimes \square\widehat{\mathsf{X}}\,| \tag{59}$$

where $A \otimes B = (A \setminus B) \cup (B \setminus A)$ and $|\cdot|$ is the cardinal for discrete sets (Eq. (58)) and the area for continuous sets (Eq. (59)). Note that Eq. (58) rewrites as

$$\mathcal{D}^{\boxdot}(\mathsf{X}, \widehat{\mathsf{X}}) = |\, \square \boxdot \mathcal{A}(\square\mathsf{X}) \otimes \square\widehat{\mathsf{X}}\,| \tag{60}$$

In other words, both digital measures can be defined via a same continuous measure as follows

$$\mathcal{D}^{\boxdot}(\mathsf{X}, \widehat{\mathsf{X}}) = \mathcal{D}(\square \boxdot \mathcal{A}(\square\mathsf{X}), \square\widehat{\mathsf{X}}) \tag{61}$$

$$\mathcal{D}^{\square}(\mathsf{X}, \widehat{\mathsf{X}}) = \mathcal{D}(\mathcal{A}(\square\mathsf{X}), \square\widehat{\mathsf{X}}) \tag{62}$$

where, for any finite $A, B \subset \mathbb{R}^2$

$$\mathcal{D}(A, B) = |\, A \otimes B\,| \tag{63}$$

Now, let us consider the complex H (that corresponds to $X_{\mathcal{A}} = \mathcal{A}(\square\mathsf{X})$) and an arbitrary complex $\widetilde{H}$ in $\mathbb{H}$. Based on the above definitions of $\mathcal{D}^{\boxdot}$ and $\mathcal{D}^{\square}$, we can derive measures $\mathcal{E}_{\text{geom}} : \mathbf{C}_{\mathbb{H}} \times \mathbf{C}_{\mathbb{H}} \to \mathbb{R}_+$ that allow us to assess the geometrical similarity between H and $\widetilde{H}$

$$\mathcal{E}^{\boxdot}_{\text{geom}}(H, \widetilde{H}) = \mathcal{D}(\square \boxdot \Pi_{\mathbb{R}^2}(H), \Pi_{\mathbb{R}^2}(\widetilde{H})) \tag{64}$$

$$\mathcal{E}^{\square}_{\text{geom}}(H, \widetilde{H}) = \mathcal{D}(\Pi_{\mathbb{R}^2}(H), \Pi_{\mathbb{R}^2}(\widetilde{H})) \tag{65}$$

Following the notations of Eq. (16) (and under the digitization constraints induced by $\mathcal{E}_{\text{digi}}$), the geometric error measures $\mathcal{E}^{\boxdot}_{\text{geom}}$ and $\mathcal{E}^{\square}_{\text{geom}}$ defined in Eqs. (64–65) in the space $\mathbb{H}$ correspond to the measures $\mathcal{D}^{\boxdot}$ and $\mathcal{D}^{\square}$ in $\mathbb{Z}^2$, respectively.

5.2 Optimization problem

5.2.1 Formulation

The complex $\widehat{H}$ we are seeking should be the solution of the following (multi-objective) optimization problem

$$\widehat{H} = \arg_{\widetilde{H} \in \mathbf{C}_{\mathbb{H}}} \min \mathcal{E}_{\text{topo}}(H, \widetilde{H}) \tag{66}$$

$$\widehat{H} = \arg_{\widetilde{H} \in \mathbf{C}_{\mathbb{H}}} \min \mathcal{E}_{\text{digi}}(\widetilde{H}) \tag{67}$$

$$\widehat{H} = \arg_{\widetilde{H} \in \mathbf{C}_{\mathbb{H}}} \min \mathcal{E}_{\text{geom}}(H, \widetilde{H}) \tag{68}$$

More precisely, we impose hard constraints on the topology (H and $\widehat{H}$ must have the same homotopy type) and on the digitization ($\widehat{H}$ must be embeddable into $\mathbb{F}$). In other words, Eqs. (66–67) must be solved exactly, i.e. we aim to have $\mathcal{E}_{\text{topo}}(H, \widehat{H}) = 0$ and $\mathcal{E}_{\text{digi}}(\widehat{H}) = 0$, whereas we accept that $\widehat{H}$ may not be optimal for Eq. (68).

5.2.2 Initialization and evolution of the error measures

The optimization process for defining $\widehat{H}$ within the cellular space $\mathbf{C}_{\mathbb{H}}$ is initialized with $\widetilde{H} = H$. In particular, at this initial stage, we have

$$\mathcal{E}_{\text{topo}}(H, H) = 0 \tag{69}$$

$$\mathcal{E}_{\text{digi}}(H) \geq 0 \tag{70}$$

$$\mathcal{E}_{\text{geom}}(H, H) \geq 0 \tag{71}$$

In other words, initially, one of the three error measures is optimized, but this is not necessarily the case for the other two, in particular $\mathcal{E}_{\text{digi}}$ that must be finally equal to 0. As a consequence, in general, H is not an acceptable solution, i.e. the identity on $\mathbf{C}_{\mathbb{H}}$ is not an acceptable solution for the sought homotopic transformation $\mathfrak{H}$.

In our process, we choose to only investigate the candidate complexes $\widetilde{H}$ that have the same homotopy type as H, i.e. that satisfy $\mathcal{E}_{\text{topo}}(\widetilde{H}, H) = 0$. In other words, we impose that $\mathcal{E}_{\text{topo}}$ remains constantly null during the whole optimization procedure. This choice is motivated by two reasons. First, as stated in Section 5.1.1, defining a topological error measure is indeed possible, but with a non-negligible

computational cost. By contrast, ensuring the topological invariance between two complexes is tractable with a negligible computational cost, for instance by considering the notion of simple cell (see Section 2.3). Second, proving that two complexes have the same homotopy type is not equivalent (in a finite space) to determining a relevant homotopic transformation between them. By contrast, building a path in the space $\mathbf{C}_{\mathbb{H}}$, composed of "successive" complexes that share the same homotopy type is indeed equivalent to building such a relevant homotopic transformation.

Regarding the other two error measures, we may have to handle antagonistic behaviours. Indeed, for $\mathcal{E}_{\text{digi}}$, we often start with a strictly positive value, and we have to reach a null value for $\widehat{H}$. By contrast, for $\mathcal{E}_{\text{geom}}$, we may start from a possibly non-optimal value, and we have to decrease as much as possible (or increase as little as possible) this value, while trying to vanish $\mathcal{E}_{\text{digi}}$ in the meantime, until reaching $\widehat{H}$.

5.3 Research space

The space $\mathbf{C}_{\mathbb{H}}$ of all the complexes on $\mathbb{H}$ has a size $2^{|\mathbb{H}_2|}$. Some of the complexes $\widetilde{H}$ of $\mathbf{C}_{\mathbb{H}}$ are such that $\Pi_{\mathbb{F}}(\widetilde{H})$ exists, i.e. they can be embedded as complexes $\widetilde{F}$ of $\mathbf{C}_{\mathbb{F}}$, and then as digital objects in $\mathbb{Z}^2$. Such complexes form a supbspace of $\mathbf{C}_{\mathbb{H}}$ noted $\mathbf{C}^{\mathbb{F}}_{\mathbb{H}}$. This subspace $\mathbf{C}^{\mathbb{F}}_{\mathbb{H}}$ is trivially isomorphic to $\mathbf{C}_{\mathbb{F}}$, and its size is $2^{|\mathbb{F}_2|}$. It is important to note that

$$\widetilde{H} \in \mathbf{C}^{\mathbb{F}}_{\mathbb{H}} \Leftrightarrow \mathcal{E}_{\text{digi}}(\widetilde{H}) = 0 \tag{72}$$

In other words, the solution $\widehat{H}$ we are seeking is necessarily a complex of $\mathbf{C}^{\mathbb{F}}_{\mathbb{H}}$.

We can endow $\mathbf{C}_{\mathbb{H}}$ with a graph structure by defining the following adjacency relation. Let H_1 and H_2 be two distinct complexes of $\mathbb{H}$. We have $H_1 \frown H_2$ iff there exists a unique 2-face $\mathfrak{h}_2 \in \mathbb{H}_2$ such that $H_1 = H_2 \circledcirc C(\mathfrak{h}_2)$. In particular, two complexes H_1 and H_2 are adjacent in the graph $(\mathbf{C}_{\mathbb{H}}, \frown)$ iff they differ from exactly one 2-cell. This graph is dense. Indeed, each complex is adjacent to $|\mathbb{H}_2|$ other complexes.

We can relevantly consider a strict subrelation of the adjacency relation $\frown$. In particular, we define the adjacency relation $\frown_h$ as follows

$$(H_1 \frown_h H_2) \Leftrightarrow \begin{cases} H_1 \frown H_2 \\ C(\mathfrak{h}_2) \text{ is a simple cell for } H_1, H_2 \end{cases} \tag{73}$$

In other words, $\frown_h$ is built from $\frown$ by considering only the couples of complexes that differ from exactly one simple cell. The induced subgraph $(\mathbf{C}_{\mathbb{H}}, \frown_h)$ is much less dense. Indeed, a complex is, most of the time, adjacent to approximately $\sqrt{|\mathbb{H}_2|}$ other complexes.

This graph $(\mathbf{C}_{\mathbb{H}}, \frown_h)$ is composed of connected components. Each connected component corresponds to a family of complexes that all share the same homotopy type.

Algorithm 1: Naive computation of $\widehat{H}$.

Input: $H \in \mathbf{C}_{\mathbb{H}}$
Input: $\mathcal{E}_{\text{geom}} : \mathbf{C}_{\mathbb{H}} \times \mathbf{C}_{\mathbb{H}} \to \mathbb{R}_+$
Output: $\widehat{H} \in \mathbf{C}^{H}_{\mathbb{H}} \cap \mathbf{C}^{\mathbb{F}}_{\mathbb{H}}$, solution of Eq. (74)

```
Ĥ initially undefined (current best solution)
(At this stage, we assume E_geom(H, Ĥ) = +∞)
H̃ initially undefined (candidate best solution)
T ← ∅ (set of tested candidate solutions)
S ← {H} (set of candidate solutions to be tested)
while S ≠ ∅ do
    Choose H̃ in S
    S ← S \ {H̃}
    T ← T ∪ {H̃}
    if E_geom(H, H̃) < E_geom(H, Ĥ) then
        if ∃F̃ ∈ C_F s.t. H̃ ≡ Π_H(F̃) then
            Ĥ ← H̃
    for all H̃_h ⌢_h H̃ do
        if H̃_h ∉ T then
            S ← S ∪ {H̃_h}
```

In particular, the connected component $\mathbf{C}^{H}_{\mathbb{H}}$ that contains H is the set of all the complexes $\widetilde{H}$ of $\mathbf{C}_{\mathbb{H}}$ which can be obtained from H via a homotopic transformation $\mathfrak{H}$ (composed by a series of attachments / detachments of simple cells, see Eq. (8)). Following the constraint that $\mathcal{E}_{\text{topo}}(\widetilde{H}, H) = 0$ during the whole optimization process, it follows that the sought optimal complex $\widehat{H}$ is an element of $\mathbf{C}^{H}_{\mathbb{H}}$.

More precisely, we have $\widehat{H} \in \mathbf{C}^{H}_{\mathbb{H}} \cap \mathbf{C}^{\mathbb{F}}_{\mathbb{H}}$, and the multi-objective optimization problem stated in Eqs. (66–68) can be refined as the following (constrained) optimization problem

$$\widehat{H} = \arg_{\widetilde{H} \in \mathbf{C}^{H}_{\mathbb{H}} \cap \mathbf{C}^{\mathbb{F}}_{\mathbb{H}}} \min \mathcal{E}_{\text{geom}}(H, \widetilde{H}) \tag{74}$$

5.4 Algorithmic aspects

5.4.1 Exhaustive approach (naive)

We are now ready to discuss on the algorithmic aspects related to the resolution of the proposed optimization problem. As stated in the above sections, our purpose is to determine a complex $\widehat{H}$ defined in the cellular space $\mathbb{H}$ that is a solution of Eqs. (66–68), and / or of Eq. (74).

A naive way of solving Eq. (74) would be to investigate all the complexes $\widetilde{H}$ that both have the same homotopy type as H and are embeddable into $\mathbb{F}$. This first approach is summarized in Algorithm 1.

This first algorithm terminates in finite time and provides the best solution $\widehat{H}$ (if it exists). However, it is not tractable in practice. Indeed, it would require to exhaustively explore the whole, potentially exponential research space $\mathbf{C}^{H}_{\mathbb{H}} \cap \mathbf{C}^{\mathbb{F}}_{\mathbb{H}}$. Nevertheless, it is relevant for discussing important details

that will be involved in the next version of algorithm actually used for solving this problem.

In particular, Algorithm 1 allows us to understand how we can explore the subspace $\mathbf{C}^H_{\mathbb{H}} \cap \mathbf{C}^{\mathbb{F}}_{\mathbb{H}}$ of $\mathbf{C}_{\mathbb{H}}$ which is composed of the complexes $\widetilde{H}$ that both have the same homotopy type as H and are embeddable into $\mathbb{F}$.

Regarding the homotopy constraints, we navigate into $\mathbf{C}^H_{\mathbb{H}}$ by starting from the initial complex H and iteratively considering complexes that successively differ from exactly one simple cell. This is the meaning of the condition $\widetilde{H}_h \frown_h \widetilde{H}$ (line 13). As discussed in Section 2.3, it is possible to characterize simple cells between two complexes (Eq. (8)) by a constant time process (see Eq. (7)). In theory, determining all the complexes $\widetilde{H}_h$ which have the same homotopy type as the complex $\widetilde{H}$ would require to investigate all the complexes that differ from $\widetilde{H}$ by exactly one cell, which would lead to a linear time cost $O(|\mathbb{H}_2|)$. In practice, based on the characterization of Eq. (7), it is sufficient to explore the complexes that differ by one cell located "on the border" of $\widetilde{H}$, which leads to a sublinear time cost, proportional to the perimeter of the complex. This notion of border can be formalized by defining the following sets of faces and cells

$$\mathbb{B}_{0,1}(\widetilde{H}) = \{\mathfrak{b}_{0,1} \in \mathbb{H}_0(\widetilde{H}) \cup \mathbb{H}_1(\widetilde{H}) \mid S(\mathfrak{b}_{0,1}) \subsetneq \widetilde{H}\} \tag{75}$$

$$\mathbb{B}_2(\widetilde{H}) = \{\mathfrak{b}_2 \in \mathbb{H}_2 \mid C(\mathfrak{b}_2) \cap \mathbb{B}_{0,1}(\widetilde{H}) \neq \emptyset\} \tag{76}$$

$$\mathbb{B}(\widetilde{H}) = \{C(\mathfrak{b}_2) \mid \mathfrak{b}_2 \in \mathbb{B}_2(\widetilde{H})\} \tag{77}$$

More precisely, in line 13, the candidate complexes $\widetilde{H}_h$ differ from $\widetilde{H}$ by exactly one 2-cell which necessarily belongs to $\mathbb{B}(\widetilde{H})$.

Regarding the embeddability of the candidate complexes $\widetilde{H}$ into $\mathbb{F}$, one can rely on Eq. (56). In other words, the information on this putative embeddability is carried by the two functions Φ and ϕ defined in Eqs. (45, 47). In addition, we can define three sets of 2-faces of $\mathbb{F}$

$$\mathbb{I}_2(\widetilde{H}) = \{\mathfrak{f}_2 \in \mathbb{F}_2 \mid \Phi(\mathfrak{f}_2) \cap \widetilde{H} = \Phi(\mathfrak{f}_2)\} \tag{78}$$

$$\mathbb{O}_2(\widetilde{H}) = \{\mathfrak{f}_2 \in \mathbb{F}_2 \mid \Phi(\mathfrak{f}_2) \cap \widetilde{H} = \emptyset\} \tag{79}$$

$$\mathbb{M}_2(\widetilde{H}) = \{\mathfrak{f}_2 \in \mathbb{F}_2 \mid \emptyset \subsetneq \Phi(\mathfrak{f}_2) \cap \widetilde{H} \subsetneq \Phi(\mathfrak{f}_2)\} \tag{80}$$

which correspond to the 2-faces of the cellular space $\mathbb{F}_2$ that lie fully inside, fully outside and both inside and outside of the complex $\widetilde{H}$, respectively.

It is possible to assess the embeddability of $\widetilde{H}$ by observing the status of $\mathbb{M}_2(\widetilde{H})$. Indeed, the condition of line 11 is equivalent to $\mathbb{M}_2(\widetilde{H}) = \emptyset$.

5.4.2 Gradient descent

We now propose a second algorithm that does not exhaustively explore the research space $\mathbf{C}^H_{\mathbb{H}} \cap \mathbf{C}^{\mathbb{F}}_{\mathbb{H}}$ and allows to reach a locally optimal solution. It relies on a gradient descent approach, and is sketched in Algorithm 2.

Algorithm 2: Computation of $\widehat{H}$.

Input: $H \in \mathbf{C}_{\mathbb{H}}$
Input: $\mathcal{E}_{\text{geom}} : \mathbf{C}_{\mathbb{H}} \times \mathbf{C}_{\mathbb{H}} \to \mathbb{R}_+$
Input: $\mathcal{E}_{\text{digi}} : \mathbf{C}_{\mathbb{H}} \to \mathbb{R}_+$
Output: $\widehat{H} \in \mathbf{C}^H_{\mathbb{H}} \cap \mathbf{C}^{\mathbb{F}}_{\mathbb{H}}$, solution of Eq. (74)

1 $\widetilde{H} \leftarrow H$
2 Build $\mathbb{B}_2(\widetilde{H})$ from Eqs. (75–76)
3 **while** $\mathcal{E}_{\text{digi}}(\widetilde{H}) > 0$ **do**
4 Choose $\mathfrak{b}_2$ in $\mathbb{B}_2(\widetilde{H})$ s.t. $\widetilde{H} \circledcirc C(\mathfrak{b}_2) \frown_h \widetilde{H}$ and minimizes $\mathcal{E}_{\text{digi}}$ and $\mathcal{E}_{\text{geom}}(H, \cdot)$
5 $\widetilde{H} \leftarrow \widetilde{H} \circledcirc C(\mathfrak{b}_2)$
6 Update $\mathbb{B}_2(\widetilde{H})$
7 $\widehat{H} \leftarrow \widetilde{H}$

If this algorithm terminates, then it is plain that the proposed solution $\widehat{H}$ satisfies Eqs. (66–67), i.e. $\widehat{H}$ has the same homotopy type as H and is embeddable into $\mathbb{F}$. The first property is ensured by the fact that for each iteration of the while loop (line 3), we select a simple cell (condition $\widetilde{H}_h \frown_h \widetilde{H}$ in line 4). The second property is ensured by the non-negativity condition in the while loop (condition $\mathcal{E}_{\text{digi}}(\widetilde{H}) > 0$ in line 3). The fact that the algorithm performs a gradient descent, i.e. that it decreases $\mathcal{E}_{\text{digi}}$ as rapidly as possible (while decreasing/increasing $\mathcal{E}_{\text{geom}}$ as slowly/rapidly as possible) depends on the choice of $\mathfrak{b}_2$ (line 4) and will be discussed hereafter.

At this stage, three important points remain to be clarified: (1) how to choose the successive 2-faces $\mathfrak{b}_2$; (2) how to guarantee (as much as possible) that the algorithm will terminate; and (3) when it terminates, how to obtain a reasonable time cost.

Based on the discussion of Section 5.4.1, we define the digitization error measure as

$$\mathcal{E}_{\text{digi}}(\widetilde{H}) = |\,\mathbb{M}_2(\widetilde{H})\,| \tag{81}$$

i.e. as the number of 2-faces of $\mathbb{F}$ that lie both inside and outside $\widetilde{H}$.

Based on the discussions of Section 5.1.3, we define the geometrical error measure as

$$\mathcal{E}_{\text{geom}}(\widehat{H}, \widetilde{H}) = \sum_{\mathfrak{b}_2 \in \mathbb{H}_2(\widehat{H}) \otimes \mathbb{H}_2(\widetilde{H})} |\mathfrak{b}_2| \tag{82}$$

where $\widehat{H} = H$ (resp. $\widehat{H} = \Pi_{\mathbb{H}}(\square \boxdot \Pi_{\mathbb{R}^2}(H))$) if one considers that $\mathcal{E}_{\text{geom}} = \mathcal{E}^{\square}_{\text{geom}}$ (resp. $\mathcal{E}_{\text{geom}} = \mathcal{E}^{\boxdot}_{\text{geom}}$). This geometrical error is equal to the area of the false positive and false negative 2-faces in $\widetilde{H}$ with respect to $\widehat{H}$.

We define an energy function ε that provides, for each 2-face $\mathfrak{b}_2$ of $\mathbb{H}$, the impact of modifying the status of $\mathfrak{b}_2$ in $\mathbb{H}$, i.e. passing from $\mathbb{H}$ to $\mathbb{H} \circledcirc C(\mathfrak{b}_2)$.

For any $\mathfrak{f}_2 \in \mathbb{F}$, we set

$$\sigma(\mathfrak{f}_2, \widehat{H}) = \begin{cases} 1 \text{ if } \sum_{\mathfrak{b}_2 \in \Phi(\mathfrak{f}_2) \cap \widehat{H}} |\mathfrak{b}_2| > 0.5 \\ -1 \text{ if } \sum_{\mathfrak{b}_2 \in \Phi(\mathfrak{f}_2) \cap \widehat{H}} |\mathfrak{b}_2| \leq 0.5 \end{cases} \tag{83}$$

In particular, $\sigma(\mathfrak{f}_2, \widehat{H})$ indicates if $\mathfrak{f}_2$ is in majority inside (1) or outside (-1) the target complex $\widehat{H}$. We also define

$$\zeta(\mathfrak{f}_2, \widehat{H}, \widetilde{H}) = \frac{1 - \sigma(\mathfrak{f}_2, \widehat{H})}{2} + \sigma(\mathfrak{f}_2, \widehat{H}) \cdot \sum_{\mathfrak{h}_2 \in \Phi(\mathfrak{f}_2) \cap \widetilde{H}} |\mathfrak{h}_2| \qquad (84)$$

In particular $\zeta(\mathfrak{f}_2, \widehat{H}, \widetilde{H})$ has a value in $[0, 1]$. If $\mathfrak{f}_2$ lies in majority inside (resp. outside) $\widehat{H}$, it gives the area of $\mathfrak{f}_2$ that lies inside (resp. outside) $\widetilde{H}$.

Then, the energy ε of a 2-face $\mathfrak{h}_2$ of $\mathbb{H}$ with respect to $\widetilde{H}$ can be defined as

$$\varepsilon(\mathfrak{h}_2, \widehat{H}, \widetilde{H}) = -\iota(\mathfrak{h}_2, \widetilde{H}) \cdot \sigma(\phi(\mathfrak{h}_2), \widehat{H}) \cdot \zeta(\phi(\mathfrak{h}_2), \widehat{H}, \widetilde{H}) \qquad (85)$$

with

$$\iota(\mathfrak{h}_2, \widetilde{H}) = \begin{cases} 1 & \text{if } \mathfrak{h}_2 \in \widetilde{H} \\ -1 & \text{if } \mathfrak{h}_2 \notin \widetilde{H} \end{cases} \qquad (86)$$

The energy function ε takes values in $[-1, 1[$. The greater this value, the higher the priority for modifying the status of the considered 2-face in order to optimize $\mathcal{E}_{\text{digi}}$ and $\mathcal{E}_{\text{geom}}$.

We can also define a topological indicator τ that provides, for each 2-face $\mathfrak{h}_2$ of $\mathbb{H}$, its simpleness status with respect to $\widetilde{H}$

$$\tau(\mathfrak{h}_2, \widetilde{H}) = \begin{cases} 1 & \text{if } C(\mathfrak{h}_2) \text{ is simple for } \widetilde{H} \\ -1 & \text{otherwise} \end{cases} \qquad (87)$$

In practice, the set $\mathbb{B}_2(\widetilde{H})$ is ordered by considering the lexicographical $\leqslant$ on $\mathbb{R}^2$, associating each 2-face $\mathfrak{h}_2$ to the couple $(\varepsilon(\mathfrak{h}_2, \widehat{H}, \widetilde{H}), \tau(\mathfrak{h}_2, \widetilde{H}))$. The face $\mathfrak{h}_2$ chosen in line 4 corresponds to the simple cell $C(\mathfrak{h}_2)$ with the maximal couple $(\varepsilon(\mathfrak{h}_2, \widehat{H}, \widetilde{H}), \tau(\mathfrak{h}_2, \widetilde{H}))$.

Following these definitions, the processing of the 2-faces $\mathfrak{h}_2$ of $\mathbb{H}_2$ is carried out "face by face" regarding the 2-faces $\mathfrak{f}_2$ of $\mathbb{F}_2$, by considering these faces from the closest to the furthest from the target complex $\widehat{H}$. This behaviour derives from the definition of ε (Eq. (85)). Doing so, the algorithm actually proceeds as a gradient descent. Indeed, it aims to optimize $\mathcal{E}_{\text{digi}}$ and $\mathcal{E}_{\text{geom}}$ as rapidly as possible.

In the favourable cases, the algorithm will terminate by processing at most once each 2-face $\mathfrak{h}_2$. The termination is characterized by the fact that the 2-face $\mathfrak{h}_2$ with the maximal couple is such that $\varepsilon(\mathfrak{h}_2, \widehat{H}, \widetilde{H}) = -1$. However, it may happen that, when processing a given 2-face $\mathfrak{f}_2$, we may be unable to reach a purity status (i.e. $\mathfrak{f}_2 \in \mathbb{M}_2$) for this face. Indeed, such non-convergence can be induced by topological deadlocks. Such a situation is characterized by the fact that the 2-face $\mathfrak{h}_2$ with the maximal couple is such that $\tau(\mathfrak{h}_2, \widetilde{H}) = -1$ while $\varepsilon(\mathfrak{h}_2, \widehat{H}, \widetilde{H}) \geq 0$. In such case, we reverse the definition of $\sigma(\mathfrak{f}_2, \widehat{H})$, i.e. we set $\sigma(\mathfrak{f}_2, \widehat{H}) \leftarrow -\sigma(\mathfrak{f}_2, \widehat{H})$ (with side effects on ζ and ε).

This reversing strategy is most of the time sufficient in order to reach a convergence of the proposed algorithm. For complexes presenting specific properties, with very small structures (e.g. very thin textures, checkerboard configurations, etc.), this gradient descent algorithm may fail, i.e. it may not converge. In particular, this non-convergence could lead to infinite iterations (line 12), due to alternating configurations. Such oscillating effects can nonetheless be easily characterized by assessing the frequency of alternating operations that every cells undergo (line 14). The optimization process can be terminated when this frequency reaches a given tolerance threshold.

Finally, it is worth mentioning that with this gradient descent algorithm, and the proposed error measure, at each step of the process, only a local updating is required, regarding the cells in the neighbourhood of the modified one, which need to be checked for simpleness characterization, and the potential addition / removal of such cells, in $\mathbb{B}_2(\widetilde{H})$ (that needs to be maintained sorted in $(\mathbb{R}^2, \leqslant)$). All these operations require, at each step of the while loop (line 3), a time $O(k \log b)$ where k is the number of cells involved in the up-

Algorithm 3: Locally optimal computation of $\widehat{H}$.

Input: $H \in \mathbf{C}_{\mathbb{H}}$
Input: $\widehat{H} \in \mathbf{C}_{\mathbb{H}}$
Output: $\widehat{H} \in \mathbf{C}^H_{\mathbb{H}} \cap \mathbf{C}^{\mathbb{F}}_{\mathbb{H}}$, solution of Eq. (74)

1 $\widetilde{H} \leftarrow H$
2 **for all** $\mathfrak{f}_2 \in \mathbb{F}_2$ **do**
3 Compute $\sigma(\mathfrak{f}_2, \widehat{H})$ (Eq. (83))
4 Compute $\zeta(\mathfrak{f}_2, \widehat{H}, \widetilde{H})$ (Eq. (84))
5 **for all** $\mathfrak{h}_2 \in \mathbb{H}_2$ **do**
6 Compute $\iota(\mathfrak{h}_2, \widetilde{H})$ (Eq. (86))
7 Compute $\varepsilon(\mathfrak{h}_2, \widehat{H}, \widetilde{H})$ (Eq. (85))
8 Compute $\tau(\mathfrak{h}_2, \widetilde{H})$ (Eq. (87))
9 Build $\mathbb{B}_2(\widetilde{H})$ (Eq. (76))
10 Sort $\mathbb{B}_2(\widetilde{H})$ in lexicograph. order $\leqslant$ wrt $(\varepsilon(\cdot, \widehat{H}, \widetilde{H}), \tau(\cdot, \widetilde{H}))$
11 $\mathfrak{h}_2^\star \leftarrow \arg\max_{\leqslant} \mathbb{B}_2(\widetilde{H})$
12 **while** $\varepsilon(\mathfrak{h}_2^\star, \widehat{H}, \widetilde{H}) \geq 0$ **do**
13 **if** $\tau(\mathfrak{h}_2^\star, \widetilde{H}) = 1$ **then**
14 $\widetilde{H} \leftarrow \widetilde{H} \circledcirc C(\mathfrak{h}_2^\star)$ (Eq. (9))
15 Update $\iota(\mathfrak{h}_2^\star, \widetilde{H})$ (Eq. (86))
16 Update $\zeta(\phi(\mathfrak{h}_2^\star), \widehat{H}, \widetilde{H})$ (Eq. (84))
17 **for all** $\mathfrak{h}_2 \in \mathbb{H}_2$ *s.t.* $C(\mathfrak{h}_2) \cap C(\mathfrak{h}_2^\star) \neq \emptyset$ **do**
18 Update $\tau(\mathfrak{h}_2, \widetilde{H})$ (Eq. (87))
19 Update / resort $\mathbb{B}_2(\widetilde{H})$ wrt $\mathfrak{h}_2$
20 **else**
21 $\sigma(\phi(\mathfrak{h}_2^\star), \widehat{H}) \leftarrow -\sigma(\phi(\mathfrak{h}_2^\star), \widehat{H})$
22 Update $\zeta(\phi(\mathfrak{h}_2^\star), \widehat{H}, \widetilde{H})$ (Eq. (84))
23 **for all** $\mathfrak{h}_2 \in \Phi(\phi(\mathfrak{h}_2^\star))$ **do**
24 Update $\varepsilon(\mathfrak{h}_2, \widehat{H}, \widetilde{H})$ (Eq. (85))
25 Update / resort $\mathbb{B}_2(\widetilde{H})$ wrt $\mathfrak{h}_2$
26 $\mathfrak{h}_2^\star \leftarrow \arg\max_{\leqslant} \mathbb{B}_2(\widetilde{H})$
27 $\widehat{H} \leftarrow \widetilde{H}$

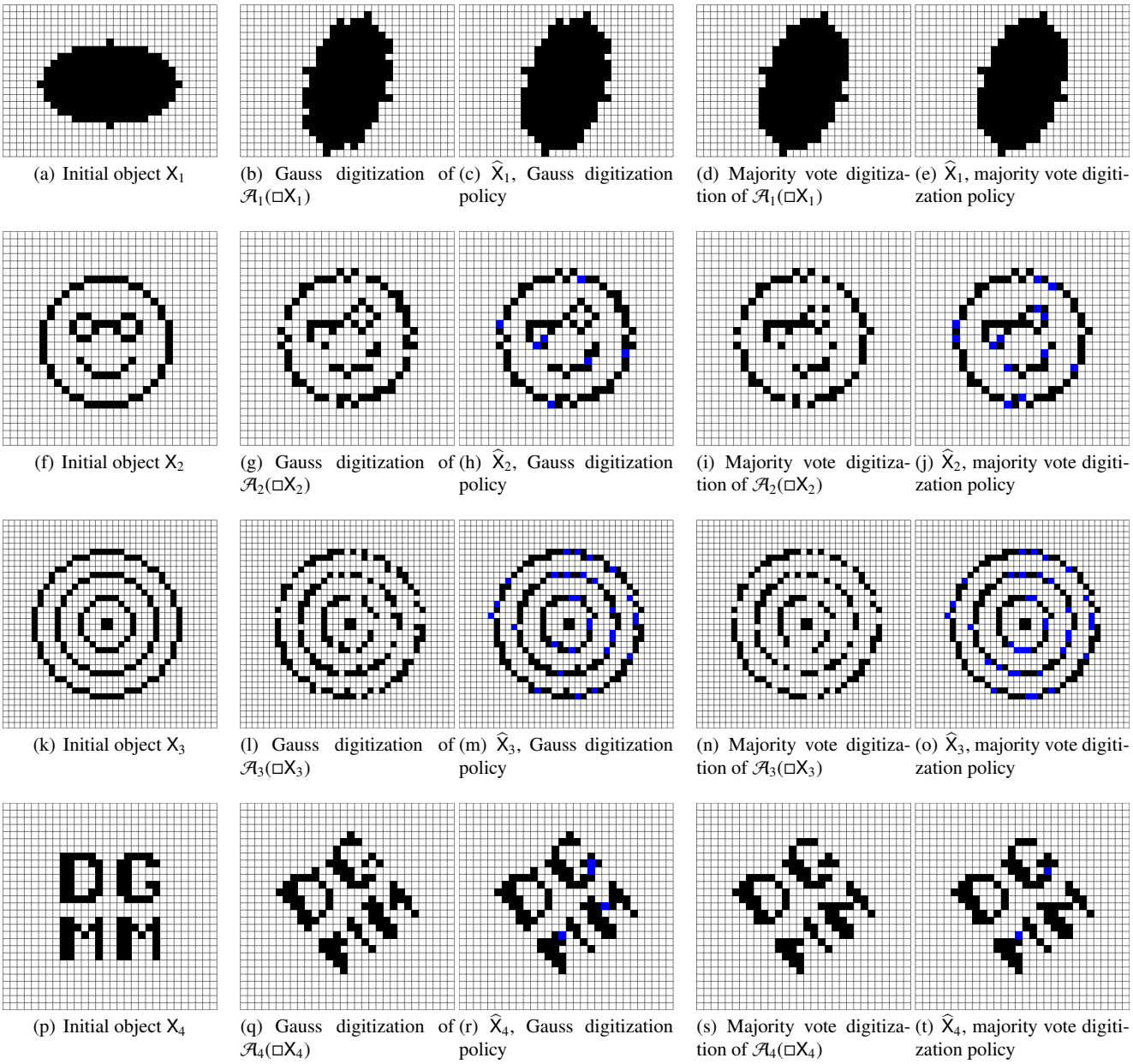

(a) Initial object X_1 (b) Gauss digitization of $\mathcal{A}_1(\square\mathsf{X}_1)$ (c) $\widehat{\mathsf{X}}_1$, Gauss digitization policy (d) Majority vote digitization of $\mathcal{A}_1(\square\mathsf{X}_1)$ (e) $\widehat{\mathsf{X}}_1$, majority vote digitization policy

(f) Initial object X_2 (g) Gauss digitization of $\mathcal{A}_2(\square\mathsf{X}_2)$ (h) $\widehat{\mathsf{X}}_2$, Gauss digitization policy (i) Majority vote digitization of $\mathcal{A}_2(\square\mathsf{X}_2)$ (j) $\widehat{\mathsf{X}}_2$, majority vote digitization policy

(k) Initial object X_3 (l) Gauss digitization of $\mathcal{A}_3(\square\mathsf{X}_3)$ (m) $\widehat{\mathsf{X}}_3$, Gauss digitization policy (n) Majority vote digitization of $\mathcal{A}_3(\square\mathsf{X}_3)$ (o) $\widehat{\mathsf{X}}_3$, majority vote digitization policy

(p) Initial object X_4 (q) Gauss digitization of $\mathcal{A}_4(\square\mathsf{X}_4)$ (r) $\widehat{\mathsf{X}}_4$, Gauss digitization policy (s) Majority vote digitization of $\mathcal{A}_4(\square\mathsf{X}_4)$ (t) $\widehat{\mathsf{X}}_4$, majority vote digitization policy

Fig. 3 Effects of rigid motions $\mathcal{A}_i$ on digital objects X_i ($1 \leq i \leq 4$). (a, f, k, p) Initial digital objects X_i. (b–e) Results of the rigid motion $\mathcal{A}_1$ on X_1 with the following parameters: $a_{11} = \frac{22}{25}, a_{12} = -\frac{7}{25}, a_{21} = \frac{22}{25}, a_{22} = \frac{7}{25}, t_x = 0, t_y = 0$ (pure rotation). (g–j) Results of the rigid motion $\mathcal{A}_2$ on X_2 with the following parameters: $a_{11} = \frac{5}{13}, a_{12} = -\frac{12}{13}, a_{21} = \frac{5}{13}, a_{22} = \frac{12}{13}, t_x = \frac{1}{5}, t_y = \frac{2}{3}$. (l–o) Results of the rigid motion $\mathcal{A}_3$ on X_3 with the following parameters: $a_{11} = \frac{3}{5}, a_{12} = -\frac{4}{5}, a_{21} = \frac{3}{5}, a_{22} = \frac{4}{5}, t_x = \frac{1}{3}, t_y = \frac{1}{3}$. (q–t) Results of the rigid motion $\mathcal{A}_4$ on X_4 with the following parameters: $a_{11} = \frac{3}{5}, a_{12} = -\frac{4}{5}, a_{21} = \frac{3}{5}, a_{22} = \frac{4}{5}, t_x = \frac{1}{5}, t_y = \frac{1}{4}$. (b, g, l, q) Results with a Gauss digitization of $\mathcal{A}_i(\square\mathsf{X}_i)$. (c, h, m, r) Results $\widehat{\mathsf{X}}_i$ with the proposed homotopic approach and Gauss digitization policy. (d, i, n, s) Results with the majority vote digitization of $\mathcal{A}_i(\square\mathsf{X}_i)$. (e, j, o, t) Results $\widehat{\mathsf{X}}_i$ with the proposed homotopic approach and majority vote digitization policy. For a given digitization (Gauss, majority vote) and a given object, X_i, the blue pixels emphasize the differences between the result obtained by digitizing $\mathcal{A}_i(\square\mathsf{X}_i)$ and the result $\widehat{\mathsf{X}}_i$ obtained with the proposed approach for the same digitization policy.

dating (generally, k is bounded by a low constant value) and b the size of $\mathbb{B}_2(\widetilde{H})$.

Algorithm 3, provides a summary of the proposed strategy and refines Algorithm 2.

6 Experiments

6.1 Topology vs. non-topology preserving transformations

Let $\mathsf{X}_\star \subset \mathbb{Z}^2$ be a digital object and $\mathcal{A}_\star : \mathbb{Q} \to \mathbb{Q}$ an affine transformation. We first compare results obtained with the

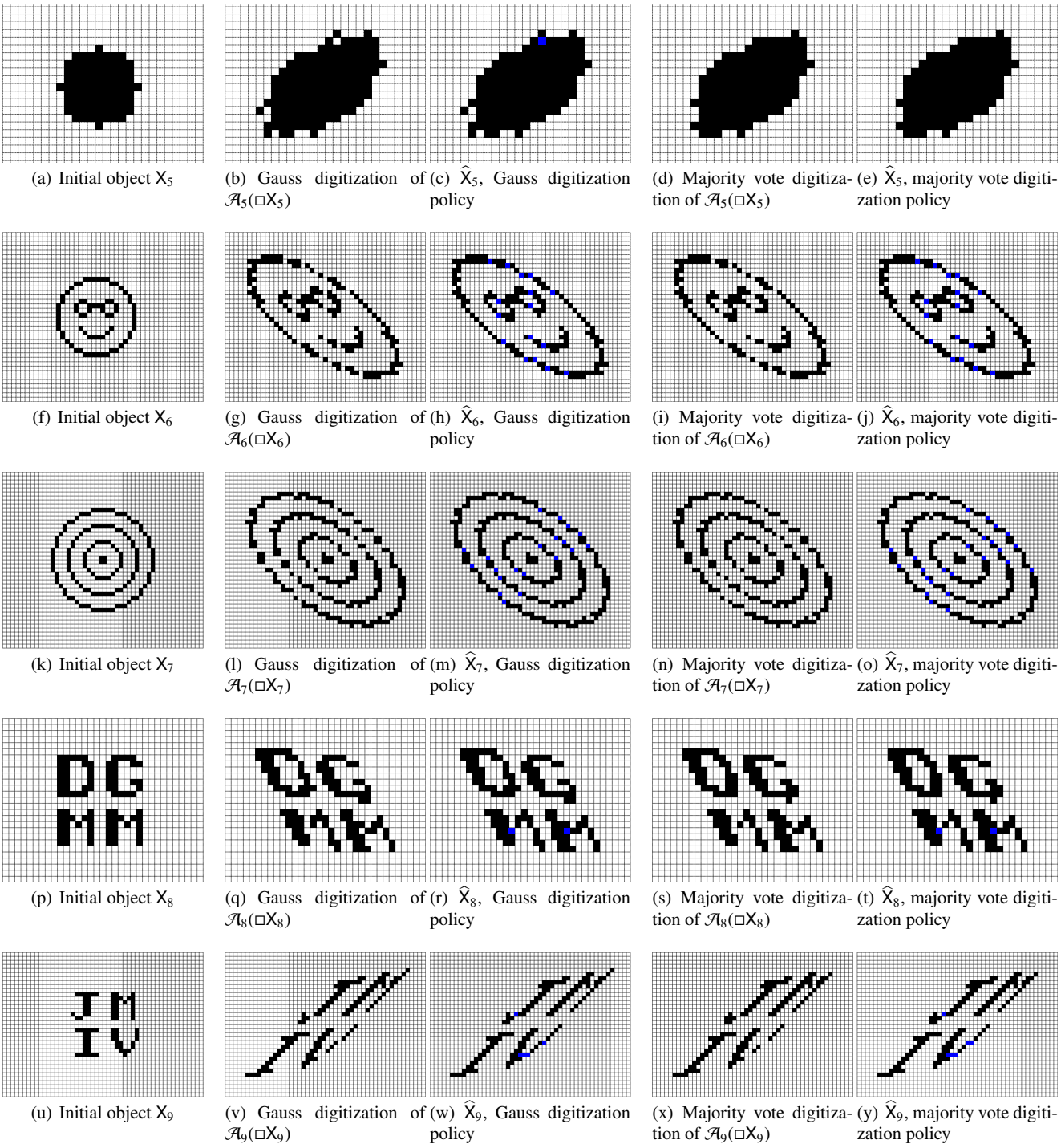

(a) Initial object X_5 (b) Gauss digitization of $\mathcal{A}_5(\square\mathsf{X}_5)$ (c) $\widehat{\mathsf{X}}_5$, Gauss digitization policy (d) Majority vote digitization of $\mathcal{A}_5(\square\mathsf{X}_5)$ (e) $\widehat{\mathsf{X}}_5$, majority vote digitization policy

(f) Initial object X_6 (g) Gauss digitization of $\mathcal{A}_6(\square\mathsf{X}_6)$ (h) $\widehat{\mathsf{X}}_6$, Gauss digitization policy (i) Majority vote digitization of $\mathcal{A}_6(\square\mathsf{X}_6)$ (j) $\widehat{\mathsf{X}}_6$, majority vote digitization policy

(k) Initial object X_7 (l) Gauss digitization of $\mathcal{A}_7(\square\mathsf{X}_7)$ (m) $\widehat{\mathsf{X}}_7$, Gauss digitization policy (n) Majority vote digitization of $\mathcal{A}_7(\square\mathsf{X}_7)$ (o) $\widehat{\mathsf{X}}_7$, majority vote digitization policy

(p) Initial object X_8 (q) Gauss digitization of $\mathcal{A}_8(\square\mathsf{X}_8)$ (r) $\widehat{\mathsf{X}}_8$, Gauss digitization policy (s) Majority vote digitization of $\mathcal{A}_8(\square\mathsf{X}_8)$ (t) $\widehat{\mathsf{X}}_8$, majority vote digitization policy

(u) Initial object X_9 (v) Gauss digitization of $\mathcal{A}_9(\square\mathsf{X}_9)$ (w) $\widehat{\mathsf{X}}_9$, Gauss digitization policy (x) Majority vote digitization of $\mathcal{A}_9(\square\mathsf{X}_9)$ (y) $\widehat{\mathsf{X}}_9$, majority vote digitization policy

Fig. 4 Effects of affine transformations $\mathcal{A}_i$ on digital objects X_i ($5 \leq i \leq 9$). (a, f, k, p, u) Initial digital objects X_i. (b–e) Results of the affine transformation $\mathcal{A}_5$ on X_5 with the following parameters: $a_{11} = \frac{3}{2}, a_{12} = \frac{1}{5}, a_{21} = \frac{1}{2}, a_{22} = \frac{6}{5}, t_x = \frac{1}{5}, t_y = \frac{1}{5}$. (g–j) Results of the affine transformation $\mathcal{A}_6$ on X_6 with the following parameters: $a_{11} = \frac{6}{5}, a_{12} = -\frac{3}{2}, a_{21} = \frac{1}{5}, a_{22} = \frac{3}{2}, t_x = \frac{1}{3}, t_y = \frac{2}{5}$. (l–o) Results of the affine transformation $\mathcal{A}_7$ on X_7 with the following parameters: $a_{11} = \frac{3}{2}, a_{12} = \frac{1}{5}, a_{21} = \frac{1}{2}, a_{22} = \frac{6}{5}, t_x = \frac{1}{2}, t_y = 0$. (q–t) Results of the affine transformation $\mathcal{A}_8$ on X_8 with the following parameters: $a_{11} = \frac{6}{5}, a_{12} = -\frac{1}{2}, a_{21} = -\frac{1}{10}, a_{22} = \frac{11}{10}, t_x = \frac{1}{2}, t_y = 0$. (v–y) Results of the affine transformation $\mathcal{A}_9$ on X_9 with the following parameters: $a_{11} = \frac{6}{5}, a_{12} = \frac{3}{2}, a_{21} = \frac{1}{5}, a_{22} = \frac{3}{2}, t_x = \frac{1}{3}, t_y = \frac{2}{5}$. (b, g, l, q, v) Results with a Gauss digitization of $\mathcal{A}_i(\square\mathsf{X}_i)$. (c, h, m, r, w) Results $\widehat{\mathsf{X}}_i$ with the proposed homotopic approach and Gauss digitization policy. (d, i, n, s, x) Results with the majority vote digitization of $\mathcal{A}_i(\square\mathsf{X}_i)$. (e, j, o, t, y) Results $\widehat{\mathsf{X}}_i$ with the proposed homotopic approach and majority vote digitization policy. For a given digitization (Gauss, majority vote) and a given object, X_i, the blue pixels emphasize the differences between the result obtained by digitizing $\mathcal{A}_i(\square\mathsf{X}_i)$ and the result $\widehat{\mathsf{X}}_i$ obtained with the proposed approach for the same digitization policy.

proposed homotopic approach that provides a result $\widehat{\mathsf{X}}_\star \subset \mathbb{Z}^2$ from the transformation of $\mathsf{X}_\star \subset \mathbb{Z}^2$ with respect to $\mathcal{A}_\star$ versus results obtained with the standard strategy that consists of carrying out $\mathcal{A}_\star$ on the continuous object $\square(\mathsf{X}_\star) \subset \mathbb{R}^2$ and then digitizing the result $\mathcal{A}_\star(\square(\mathsf{X}_\star)) \subset \mathbb{R}^2$ to come back to $\mathbb{Z}^2$. Such results are illustrated in Figure 3 for four couples of objects X_i and rigid transformations $\mathcal{A}_i$ ($1 \leq i \leq 4$) and in Figure 4 for five couples of objects X_i and more general affine transformations $\mathcal{A}_i$ ($5 \leq i \leq 9$). In both figures, we investigate the behaviour of two digitizations, namely the Gauss digitization and the majority vote digitization.

We first consider simple objects, with a trivial topology (one connected component, no hole), namely an ellipse X_1 (Figure 3(a)) and disk X_5 (Figure 4(a)). In the case of a rigid transformation $\mathcal{A}_1$, the topology is preserved here for both the standard approach (Figure 3(b, d)) and our strategy (Figure 3(c, e)), and the results are the same. This emphasizes the compliance of our approach with the standard one when there is no topological defect has to be corrected. This behaviour was expected; indeed, in absence topological deadlock (i.e. when the condition of line 13 in Algorithm 3 is always true), the gradient descent algorithm converges onto a result that corresponds to the globally optimal solution for $\mathcal{E}_{\text{geom}}$. In particular, we then have

$$\mathcal{E}^{\square}_{\text{geom}}(H, \widehat{H}) = 0 \tag{88}$$

$$\mathcal{E}^{\square}_{\text{geom}}(H, \widehat{H}) = \sum_{\mathfrak{f}_2 \in \mathbb{M}_2(H)} \min \left\{ \sum_{\mathfrak{b}_2 \in \Phi(\mathfrak{f}_2) \cap H} |\mathfrak{b}_2|, 1 - \sum_{\mathfrak{b}_2 \in \Phi(\mathfrak{f}_2) \cap H} \right\} \tag{89}$$

which are the optimal values that can be reached.

Even for such simple objects, we observe however that for more general affine transformations such as $\mathcal{A}_5$, the standard strategy can lead to topological defects, here the creation of a hole (Figure 4(b)). In this context, our approach is able to deal with this issue (Figure 4(c)), and the topology is then preserved.

For more complex objects X_i (i = 2–4, 6–9) (Figures 3(f, k, p) and 4(f, k, p, u)) with many connected components and many holes (possibly small/thin), for both rigid transformations and affine transformations, and for both Gauss and majority vote digitization, the standard strategy leads to many topological defects (disconnections) (Figures 3(g, i, l, n, q, s) and 4(g, i, l, n, q, s, v, x)). By contrast, our proposed approach is able to correctly handle the topological constraints, leading to to transformed objects with the same homotopy type as the initial objects (Figures 3(h, j, m, o, r, t) and 4(h, j, m, o, r, t, w, y)). Once again, this was expected, since the homotopy type is preserved by construction.

It is important to note that these results are geometrically fairly close to the "standard". The differences between both are emphasized by the pixels in blue in Figures 3 and 4. In particular, one can observe that in all the cases (except one pixel in Figure 3(o)), the pixels that differ between the results of our approach and the standard results are only those which are mandatory to guarantee the preservation of the homotopy type. In other words, in these experiments, although a globally optimal value of $\mathcal{E}_{\text{geom}}$ cannot be reached due to topological constraints, it is generally optimized as much as possible.

6.2 Comparison of topology preserving transformations

We now compare results obtained with different methods for topology preserving geometric transformations, relying on the following paradigms:

- the notion of (digital) regularity [43] defined for identifying a class of two-dimensional digital images, that preserve the 4-connectedness and well-composedness [32] of digital images;
- the notion of quasi-regularity [42] defined for identifying a class of polygons, that preserve the 4-connectedness and well-composedness of digitized polygons;
- the proposed approach.

To this end, we consider three digital objects:

1. $\mathsf{X}_{10} \subset \mathbb{Z}^2$ which is (digitally) regular and generated as the Gauss digitization of a quasi-regular polygon $P_{10} \subset \mathbb{R}^2$;
2. $\mathsf{X}_{11} \subset \mathbb{Z}^2$ which is not (digitally) regular (but 4-connected and well-composed) and is generated as the Gauss digitization of a quasi-regular polygon $P_{11} \subset \mathbb{R}^2$;
3. $\mathsf{X}_{12} \subset \mathbb{Z}^2$ which is not (digitally) regular and generated as the Gauss digitization of a non-quasi-regular polygon $P_{12} \subset \mathbb{R}^2$.

The results of these experiments are illustrated in Figure 5.

These examples emphasize the ability of the different approaches to preserve the topology when the required properties are satisfied. The digitization of a quasi-regular polygon (Figure 5(a, b)) remains 4-connected and well-composed after a rigid transformation. A (digitally) regular object (Figure 5(a)) also remains 4-connected and well-composed after a rigid transformation.

However, when the required properties are no longer satisfied, the notions of (digital) regularity and quasi-regularity do not preserve their associated topological properties. For instance, in Figure 5(b), a (digitally) non-regular object is neither 4-connected nor well-composed after the transformation in Figure 5(h)). In Figure 5(c) a (digitally) non-regular object and the digitization of a non-quasi-regular polygon undergo disconnections and/or erroneous connections after the transformations in Figure 5(i, l)).

In all these cases, our proposed approach is able to preserve the topology, here the preservation of the 8-connectedness.

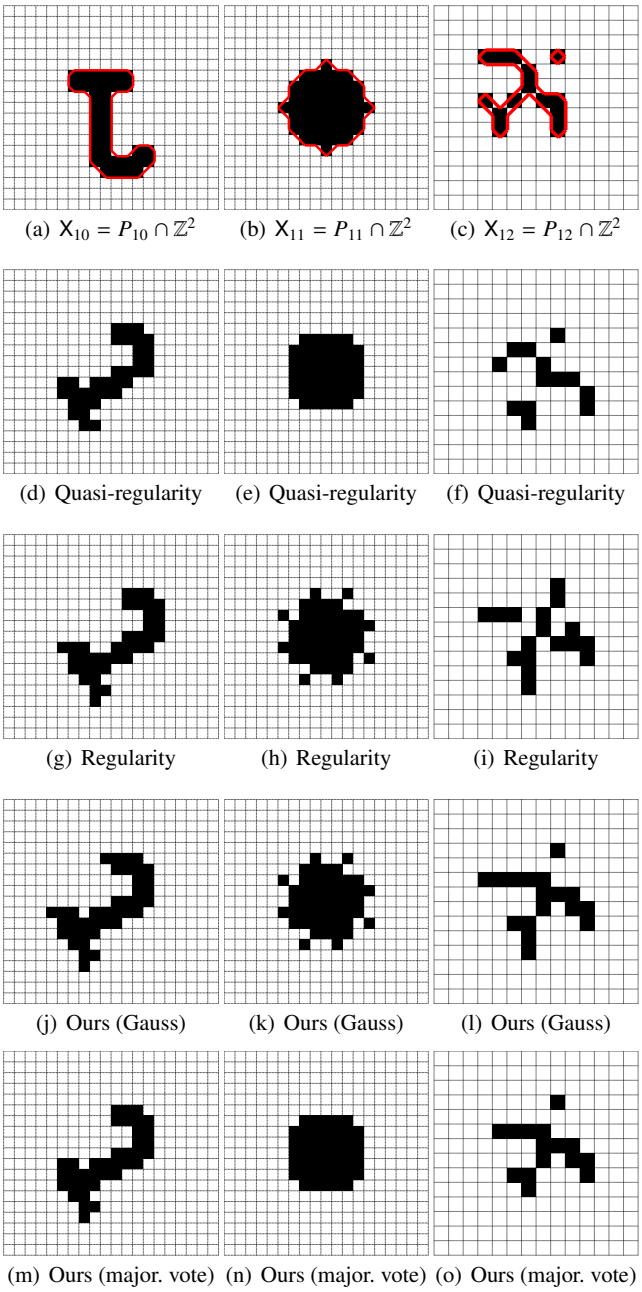

(a) $\mathsf{X}_{10} = P_{10} \cap \mathbb{Z}^2$ (b) $\mathsf{X}_{11} = P_{11} \cap \mathbb{Z}^2$ (c) $\mathsf{X}_{12} = P_{12} \cap \mathbb{Z}^2$

(d) Quasi-regularity (e) Quasi-regularity (f) Quasi-regularity

(g) Regularity (h) Regularity (i) Regularity

(j) Ours (Gauss) (k) Ours (Gauss) (l) Ours (Gauss)

(m) Ours (major. vote) (n) Ours (major. vote) (o) Ours (major. vote)

Fig. 5 (a–c) Digital objects X_i and associated polygons P_i, such that $\mathsf{X}_i = P_i \cap \mathbb{Z}^2$ ($10 \leq i \leq 12$). The digital objects X_i are (digitally) regular in (a) and (digitally) non-regular in (b, c). The polygons P_i are quasi-regular in (a, b) and non-quasi-regular in (c). (d–o) Results for the rigid transformations $\mathcal{A}_i$: (d,g,j,m) $\mathcal{A}_{10}$ (rotation angle: $\frac{2\pi}{3}$); (e,h,k,n) $\mathcal{A}_{11}$ (rotation angle: $\frac{3\pi}{8}$); (f,i,l,o) $\mathcal{A}_{12}$ (rotation angle: $\frac{\pi}{9}$). (d–f) Results based on the quasi-regularity paradigm. (g–i) Results based on the (digital) regularity paradigm. (j–l) Result based on the proposed method, with a Gauss digitization policy. (m–o) Result based on the proposed method, with a majority vote digitization policy.

These experiments are carried out only for rigid transformations, since the notions of (digital) regularity and quasi-regularity are defined only in this context. It is worth noting that the notion of (digital) regularity requires in particular that the object is well-composed and has no isolated point, while quasi-regularity requires (with its current formulation) that the digitized object is simply connected. Such requirements are not mandatory with the proposed approach, which is then more versatile.

It is also to be noticed that the notions of (digital) regularity and quasi-regularity deal with Gauss digitization only, whereas the proposed approach can handle a wider range of digitizations, since the digitization policy can be embedded in the metrics to be optimized.

7 Conclusion

In this article, we proposed an optimization strategy dedicated to compute the result of an affine transformation applied on a digital object with the constraint of preserving its topology while altering as little as possible its geometry. From a structural point of view, this approach relies on the embedding of the digital object in cellular spaces, which allows us to benefit simultaneously from both continuous and discrete properties. From an algorithmic point of view, we rely on an optimization strategy, where the evolution of an initial model towards the expected solution is guided and constrained by three kinds of measures, that deal with topology, geometry and digitization information.

The proposed strategy, discussed in Section 5.4.2 and summarized in Algorithm 3 can be seen as a gradient descent approach, that preserves the homotopy type during its whole processing, and aims to progressively optimize the digitization and geometrical measures, with the purpose to reach the actually optimal value for the first and a value as optimal as possible for the second.

When this process terminates, it gives a result which is a local optimum for the proposed problem. For most of the digital objects usually handled in discrete geometry, this optimum is indeed the global one. This is, for instance, the case in the examples considered in Section 6.

However, for more complex objects, and especially for those with very textured details that lie at the limit of resolution of the grid (e.g. a checkerboard with one-pixel-sized connected components), it may happen that the proposed algorithm provides a non-globally optimal result, or even fail to terminate. In order to deal with such issues, it will be necessary to consider more general optimization strategies that could explore more deeply the research space than a standard gradient descent. The development of such strategies constitutes our short-term perspectives.

As mid-term perspectives, we will also investigate our approach with other kinds of topological models (e.g. the well-composed sets [32]), but also with non-binary images [15,35]. Longer-term perspectives will consist of investigating transformations in higher dimensions.

Acknowledgements

This work was supported by the French *Agence Nationale de la Recherche* (Grants ANR-15-CE23-0009, ANR-15-CE40-0006 and ANR-18-CE23-0025).

References

1. Amir, A., Butman, A., Lewenstein, M., Porat, E.: Real two dimensional scaled matching. Algorithmica **53**, 314–336 (2009)
2. Amir, A., Kapah, O., Tsur, D.: Faster two-dimensional pattern matching with rotations. Theoretical Computer Science **368**, 196–204 (2006)
3. Amir, A., Landau, G.M., Vishkin, U.: Efficient pattern matching with scaling. Journal of Algorithms **13**, 2–32 (1992)
4. Andres, É.: The quasi-shear rotation. In: DGCI. pp. 307–314 (1996)
5. Andres, É., Dutt, M., Biswas, A., Largeteau-Skapin, G., Zrour, R.: Digital two-dimensional bijective reflection and associated rotation. In: DGCI. pp. 3–14 (2019)
6. Anglin, W.S.: Using Pythagorean triangles to approximate angles. American Mathematical Monthly **95**, 540–541 (1988)
7. Baudrier, É., Mazo, L.: Combinatorics of the Gauss digitization under translation in 2D. Journal of Mathematical Imaging and Vision **61**, 224–236 (2019)
8. Berthé, V., Nouvel, B.: Discrete rotations and symbolic dynamics. Theoretical Computer Science **380**, 276–285 (2007)
9. Bertrand, G., Malandain, G.: A new characterization of three-dimensional simple points. Pattern Recognition Letters **15**, 169–175 (1994)
10. Bloch, I., Pescatore, J., Garnero, L.: A new characterization of simple elements in a tetrahedral mesh. Graphical Models **67**, 260–284 (2005)
11. Blot, V., Coeurjolly, D.: Quasi-affine transformation in higher dimension. In: DGCI. pp. 493–504 (2009)
12. Breuils, S., Kenmochi, Y., Sugimoto, A.: Visiting bijective digitized reflections and rotations using geometric algebra. In: DGMM. pp. 242–254 (2021)
13. Coeurjolly, D., Blot, V., Jacob-Da Col, M.A.: Quasi-affine transformation in 3-D: Theory and algorithms. In: IWCIA. pp. 68–81 (2009)
14. Couprie, M., Bertrand, G.: New characterizations of simple points in 2D, 3D, and 4D discrete spaces. IEEE Transactions on Pattern Analysis and Machine Intelligence **31**, 637–648 (2009)
15. Couprie, M., Nivando Bezerra, F., Bertrand, G.: Topological operators for grayscale image processing. Journal of Electronic Imaging **10**, 1003–1015 (2001)
16. Damiand, G., Dupas, A., Lachaud, J.O.: Fully deformable 3D digital partition model with topological control. Pattern Recognition Letters **32**, 1374–1383 (2011)
17. Faisan, S., Passat, N., Noblet, V., Chabrier, R., Meyer, C.: Topology preserving warping of 3-D binary images according to continuous one-to-one mappings. IEEE Transactions on Image Processing **20**, 2135–2145 (2011)
18. Guihéneuf, P.: Discretizations of isometries. In: DGCI. pp. 71–92 (2016)
19. Han, X., Xu, C., Prince, J.L.: A topology preserving level set method for geometric deformable models. IEEE Transactions on Pattern Analysis and Machine Intelligence **25**, 755–768 (2003)
20. Heijmans, H.J.A.M., Ronse, C.: The algebraic basis of mathematical morphology. I Dilations and erosions. Computer Vision, Graphics, and Image Processing **50**, 245–295 (1990)
21. Hundt, C.: Affine image matching is uniform TC^0-complete. In: CPM. pp. 13–25 (2010)
22. Hundt, C., Liśkiewicz, M., Ragnar, N.: A combinatorial geometrical approach to two-dimensional robust pattern matching with scaling and rotation. Theoretical Computer Science **410**, 5317–5333 (2009)
23. Hundt, C., Liskiewicz, M.: On the complexity of affine image matching. In: STACS. pp. 284–295 (2007)
24. Jacob, M.A.: Transformation of digital images by discrete affine applications. Computers & Graphics **19**, 373–389 (1995)
25. Jacob, M.A., Andres, É.: On discrete rotations. In: DGCI. pp. 161–174 (1995)
26. Jacob-Da Col, M.A.: Applications quasi-affines et pavages du plan discret. Theoretical Computer Science **259**, 245–269 (2001)
27. Jacob-Da Col, M.A., Tellier, P.: Quasi-linear transformations and discrete tilings. Theoretical Computer Science **410**, 2126–2134 (2009)
28. Jacob-Da Col, M.A., Tellier, P.: Quasi-linear transformations, numeration systems and fractals. In: DGCI. pp. 187–198 (2011)
29. Jacob-Da Col, M., Mazo, L.: nD quasi-affine transformations. In: DGCI. pp. 337–348 (2016)
30. Klette, R., Rosenfeld, A.: Digital Geometry: Geometric Methods for Digital Picture Analysis. Elsevier, Amsterdam, Boston (2004)
31. Kovalevsky, V.A.: Finite topology as applied to image analysis. Computer Vision, Graphics, and Image Processing **46**, 141–161 (1989)
32. Latecki, L.J., Eckhardt, U., Rosenfeld, A.: Well-composed sets. Computer Vision and Image Understanding **61**, 70–83 (1995)
33. Mazo, L., Baudrier, É.: Object digitization up to a translation. Journal of Computer and System Sciences. **95**, 193–203 (2018)
34. Mazo, L., Passat, N., Couprie, M., Ronse, C.: Paths, homotopy and reduction in digital images. Acta Applicandae Mathematicae **113**, 167–193 (2011)
35. Mazo, L., Passat, N., Couprie, M., Ronse, C.: Topology on digital label images. Journal of Mathematical Imaging and Vision **44**, 254–281 (2012)
36. Mazo, L., Passat, N., Couprie, M., Ronse, C.: Digital imaging: A unified topological framework. Journal of Mathematical Imaging and Vision **44**, 19–37 (2012)
37. Nehlig, P.: Applications quasi affines : pavages par images réciproques. Theoretical Computer Science **156**, 1–38 (1996)
38. Ngo, P., Kenmochi, Y., Passat, N., Talbot, H.: Combinatorial structure of rigid transformations in 2D digital images. Computer Vision and Image Understanding **117**, 393–408 (2013)
39. Ngo, P., Kenmochi, Y., Passat, N., Talbot, H.: Topology-preserving conditions for 2D digital images under rigid transformations. Journal of Mathematical Imaging and Vision **49**, 418–433 (2014)
40. Ngo, P., Kenmochi, Y., Passat, N., Talbot, H.: On 2D constrained discrete rigid transformations. Annals of Mathematics and Artificial Intelligence **75**, 163–193 (2015)
41. Ngo, P., Passat, N., Kenmochi, Y., Debled-Rennesson, I.: Convexity invariance of voxel objects under rigid motions. In: ICPR. pp. 1157–1162 (2018)
42. Ngo, P., Passat, N., Kenmochi, Y., Debled-Rennesson, I.: Geometric preservation of 2D digital objects under rigid motions. Journal of Mathematical Imaging and Vision **61**, 204–223 (2019)
43. Ngo, P., Passat, N., Kenmochi, Y., Talbot, H.: Topology-preserving rigid transformation of 2D digital images. IEEE Transactions on Image Processing **23**, 885–897 (2014)
44. Nouvel, B., Rémila, E.: Characterization of bijective discretized rotations. In: IWCIA. pp. 248–259 (2004)
45. Nouvel, B., Rémila, E.: Incremental and transitive discrete rotations. In: IWCIA. pp. 199–213 (2006)
46. Passat, N., Kenmochi, Y., Ngo, P., Pluta, K.: Rigid motions in the cubic grid: A discussion on topological issues. In: DGCI. pp. 127–140 (2019)
47. Passat, N., Ngo, P., Kenmochi, Y.: Homotopic digital rigid motion: An optimization approach on cellular complexes. In: DGMM. pp. 189–201 (2021)

48. Pluta, K., Moroz, G., Kenmochi, Y., Romon, P.: Quadric arrangement in classifying rigid motions of a 3D digital image. In: CASC. pp. 426–443 (2016)
49. Pluta, K., Romon, P., Kenmochi, Y., Passat, N.: Bijectivity certification of 3D digitized rotations. In: CTIC. pp. 30–41 (2016)
50. Pluta, K., Romon, P., Kenmochi, Y., Passat, N.: Bijective digitized rigid motions on subsets of the plane. Journal of Mathematical Imaging and Vision **59**, 84–105 (2017)
51. Rosenfeld, A.: Adjacency in digital pictures. Information and Control **26**, 24–33 (1974)
52. Rosenfeld, A.: Digital topology. The American Mathematical Monthly **86**, 621–630 (1979)
53. Rosenfeld, A., Kong, T.Y., Nakamura, A.: Topology-preserving deformations of two-valued digital pictures. Graphical Models and Image Processing **60**, 24–34 (1998)
54. Roussillon, T., Coeurjolly, D.: Characterization of bijective discretized rotations by Gaussian integers. Tech. rep. (2016), `https://hal.archives-ouvertes.fr/hal-01259826`
55. Saha, P.K., Chaudhuri, B.B., Chanda, B., Majumder, D.D.: Topology preservation in 3D digital space. Pattern Recognition **27**, 295–300 (1994)
56. Thibault, Y., Sugimoto, A., Kenmochi, Y.: 3D discrete rotations using hinge angles. Theoretical Computer Science **412**, 1378–1391 (2011)
57. Whitehead, J.H.C.: Simplicial spaces, nuclei and m-groups. Proceedings of the London Mathematical Society **s2-45**, 243–327 (1939)

A Construction of the cellular space $\mathbb{H}$

We describe hereafter the way we build the cellular space $\mathbb{H}$ that refines the two cubical spaces $\mathbb{F}$ and $\mathbb{G}$.

A.1 Input

Although $\mathbb{F}$, $\mathbb{G}$ and $\mathbb{H}$ are infinite spaces, our purpose is to handle finite digital objects. As a consequence, our first input is a finite subset S of $\mathbb{Z}^2$ that will include these digital objects. Without loss of generality, we assume that

$$\mathsf{S} = [\![-s, s]\!]^2 \subset \mathbb{Z}^2 \tag{90}$$

is a square with $s \in \mathbb{N}^\star$. The continuous analogue of this digital set S is the Euclidean square subset of $\mathbb{R}^2$ defined as

$$S = \square\mathsf{S} = [-s - \frac{1}{2}, s + \frac{1}{2}]^2 \subset \mathbb{R}^2 \tag{91}$$

The parameters that define the affine transformation $\mathcal{A}$ are also required, namely the values $a_{11}, a_{12}, a_{21}, a_{22}, t_x, t_y \in \mathbb{Q}$ (see Eq. (2)). Consequently, the information required as input is a 7-uple $(s, a_{11}, a_{12}, a_{21}, a_{22}, t_x, t_y) \in \mathbb{N}^\star \times \mathbb{Q}^6$.

A.2 Output

The output of the algorithm is the finite subspace (namely a complex) of the cellular space $\mathbb{H}$ that intersects a Euclidean square

$$Q = [q_x, q_x + w] \times [q_y, q_y + w] \subset \mathbb{R}^2 \tag{92}$$

with $\mathbf{q} \in (\mathbb{Z} + \frac{1}{2})^2$ and $w \in \mathbb{N}^\star$.

The output cellular space

$$\mathbb{H}(Q) = \{\mathfrak{h} \in \mathbb{H} \mid \mathfrak{h} \subset Q\} \tag{93}$$

is defined as a finite set of faces of $\mathbb{H}$, and is partitioned into three subsets $\mathbb{H}_0(Q)$, $\mathbb{H}_1(Q)$ and $\mathbb{H}_2(Q)$ that contain the 0-, 1- and 2-faces of $\mathbb{H}(Q)$, respectively. In particular, $\mathbb{H}_0(Q) \cup \mathbb{H}_1(Q) \cup \mathbb{H}_2(Q) = \mathbb{H}(Q)$ is a partition of Q.

For each face $\mathfrak{h}$, we also compute the closure $C(\mathfrak{h})$ and/or the star $S(\mathfrak{h})$ within the subspace $\mathbb{H}(Q)$. If $\mathfrak{h}$ is a 0- (resp. 1-, resp. 2-) face, we compute $S_1(\mathfrak{h})$ and $S_2(\mathfrak{h})$ (resp. $C_0(\mathfrak{h})$ and $S_2(\mathfrak{h})$, resp. $C_0(\mathfrak{h})$ and $C_1(\mathfrak{h})$) where $S_d(\mathfrak{h})$ (resp. $C_d(\mathfrak{h})$) is the part of $S(\mathfrak{h})$ (resp. $C(\mathfrak{h})$) composed by the d-faces ($0 \leq d \leq 2$).

For each 2-face $\mathfrak{h}_2$, we also compute the functions ϕ and γ. More precisely, we compute the functions $\widetilde{\phi}, \widetilde{\gamma} : \mathbb{H}_2 \to \mathbb{Z}^2$ such that

$$\widetilde{\phi}(\mathfrak{h}_2) = \square(\phi(\mathfrak{h}_2)) \tag{94}$$

$$\widetilde{\gamma}(\mathfrak{h}_2) = \square(\mathcal{A}^{-1}(\gamma(\mathfrak{h}_2))) \tag{95}$$

This is indeed relevant since $\square$ is a bijection between $\mathbb{F}_2$ and $\mathbb{Z}^2$ while $\square \circ \mathcal{A}^{-1}$ is a bijection between $\mathbb{G}_2$ and $\mathbb{Z}^2$. In particular, these functions allow us to define the two functions $\widetilde{\Phi} : \square Q \subset \mathbb{Z}^2 \to 2^{\mathbb{H}_2}$ and $\widetilde{\Gamma} : \mathsf{S} \subset \mathbb{Z}^2 \to 2^{\mathbb{H}_2}$ such that for any $\mathbf{p} \in \phi(\mathbb{H}_2)$ (resp. $\mathbf{p} \in \mathsf{S}$), we have $\widetilde{\Phi}(\mathbf{p}) = \widetilde{\phi}^{-1}(\{\mathbf{p}\})$ (resp. $\widetilde{\Gamma}(\mathbf{p}) = \widetilde{\gamma}^{-1}(\{\mathbf{p}\})$).

A.3 Definition of the square Q

The first task is to define the square Q, i.e. to define $\mathbf{q}$ and w so that Q includes the image of the square S by the affine transformation $\mathcal{A}$. Since S is convex, we can simply compute the images of the four vertices of S by $\mathcal{A}$ to reach that goal. In particular, for $0 \leq i, j \leq 1$, we set

$$\mathbf{c}^{i,j} = ((-1)^i(s + \frac{1}{2}), (-1)^j(s + \frac{1}{2})) \tag{96}$$

The four points $\mathbf{c}^{i,j}$ are the vertices of S. For $0 \leq i, j \leq 1$, we compute $\mathbf{r}^{i,j} = \mathcal{A}(\mathbf{c}^{i,j})$. We set

$$r_x^- = \min_{i,j}\{\lfloor r_x^{i,j} + \frac{1}{2} \rfloor\} - \frac{1}{2} \tag{97}$$

$$r_y^- = \min_{i,j}\{\lfloor r_y^{i,j} + \frac{1}{2} \rfloor\} - \frac{1}{2} \tag{98}$$

$$r_x^+ = \max_{i,j}\{\lceil r_x^{i,j} - \frac{1}{2} \rceil\} + \frac{1}{2} \tag{99}$$

$$r_y^+ = \max_{i,j}\{\lceil r_y^{i,j} - \frac{1}{2} \rceil\} + \frac{1}{2} \tag{100}$$

Finally, we define

$$q_x = r_x^- \tag{101}$$

$$q_y = r_y^- \tag{102}$$

$$w = \max\{r_x^+ - r_x^-, r_y^+ - r_y^-\} \tag{103}$$

The square Q is then defined by its four vertices $\mathbf{q}^{0,0} = \mathbf{q}$, $\mathbf{q}^{w,0} = \mathbf{q} + w\mathbf{e}_x$, $\mathbf{q}^{0,w} = \mathbf{q} + w\mathbf{e}_y$ and $\mathbf{q}^{w,w} = \mathbf{q} + w\mathbf{e}_x + w\mathbf{e}_y$.

A.4 Definition of the generator lines of $\mathbb{H}(Q)$

The cellular subspace $\mathbb{H}(Q)$ is induced by the subdivision of Q by the lines of $\mathscr{V}_\Delta$, $\mathscr{H}_\Delta$, $\mathcal{A}(\mathscr{V}_\Delta)$ and $\mathcal{A}(\mathscr{H}_\Delta)$. These four sets are infinite, but for each of them, the subset of lines that contribute to the subdivision of Q is finite and corresponds to the lines that intersect the square Q. The subsets $\mathscr{V}_\Delta(Q)$ of $\mathscr{V}_\Delta$ and $\mathscr{H}_\Delta(Q)$ of $\mathscr{H}_\Delta$ are defined by

$$\mathscr{V}_\Delta(Q) = \{V_\delta \mid \delta \in \Delta \cap [q_x, q_x + w]\} \tag{104}$$

$$\mathscr{H}_\Delta(Q) = \{H_\delta \mid \delta \in \Delta \cap [q_y, q_y + w]\} \tag{105}$$

while the subsets $\mathcal{A}(\mathscr{V}_\Delta)(Q)$ of $\mathcal{A}(\mathscr{V}_\Delta)$ and $\mathcal{A}(\mathscr{H}_\Delta)(Q)$ of $\mathcal{A}(\mathscr{H}_\Delta)$ can be determined as follows. For $0 \leq i, j \leq 1$, we compute

$$\mathbf{u}^{i,j} = \mathcal{A}^{-1}(\mathbf{q}^{iw,jw}) \tag{106}$$

These four points $\mathbf{u}^{i,j}$ are the vertices of the parallelogram $\mathcal{A}^{-1}(Q)$. We set

$$\delta_x^- = \min_{i,j}(\lceil u_x^{i,j} + \frac{1}{2} \rceil) - \frac{1}{2} \tag{107}$$

$$\delta_x^+ = \max_{i,j}(\lfloor u_x^{i,j} - \frac{1}{2} \rfloor) + \frac{1}{2} \tag{108}$$

$$\delta_y^- = \min_{i,j}(\lceil u_y^{i,j} + \frac{1}{2} \rceil) - \frac{1}{2} \tag{109}$$

$$\delta_y^+ = \max_{i,j}(\lfloor u_y^{i,j} - \frac{1}{2} \rfloor) + \frac{1}{2} \tag{110}$$

The only lines of $\mathscr{V}_\Delta$ (resp. $\mathscr{H}_\Delta$) that intersect $\mathcal{A}^{-1}(Q)$ are the lines V_δ (resp. H_δ) for $\delta_x^- \leq \delta \leq \delta_x^+$ (resp. $\delta_y^- \leq \delta \leq \delta_y^+$). This leads us to define the subsets $\mathcal{A}(\mathscr{V}_\Delta)(Q)$ of $\mathcal{A}(\mathscr{V}_\Delta)$ and $\mathcal{A}(\mathscr{H}_\Delta)(Q)$ of $\mathcal{A}(\mathscr{H}_\Delta)$ as follows

$$\mathcal{A}(\mathscr{V}_\Delta)(Q) = \{\mathcal{A}(V_\delta) \mid \delta_x^- \leq \delta \leq \delta_x^+\} \tag{111}$$

$$\mathcal{A}(\mathscr{H}_\Delta)(Q) = \{\mathcal{A}(H_\delta) \mid \delta_y^- \leq \delta \leq \delta_y^+\} \tag{112}$$

A.5 Definition of $\mathbb{H}_0(Q)$

Any 0-face $\mathfrak{f}_0$ of $\mathbb{H}(Q)$ corresponds to the intersection of (at least) two lines of $\mathscr{V}_\Delta(Q)$, $\mathscr{H}_\Delta(Q)$, $\mathcal{A}(\mathscr{V}_\Delta)(Q)$ and $\mathcal{A}(\mathscr{H}_\Delta)(Q)$ inside the square Q. (Of course, such two lines cannot belong to a same subset.) Reversely, two lines from two of these subsets can induce at most one such 0-face. In order to ensure that the intersection between two lines is indeed inside the square Q, we define for each line L the segment, noted $Q(L)$, that corresponds the intersection between L and Q. In particular, two lines L_1 and L_2 will intersect inside Q iff $Q(L_1)$ and $Q(L_2)$ intersect.

Let L be a line of $\mathscr{V}_\Delta(Q)$, $\mathscr{H}_\Delta(Q)$, $\mathcal{A}(\mathscr{V}_\Delta)(Q)$ or $\mathcal{A}(\mathscr{H}_\Delta)(Q)$. We compute the putative intersections

$$L \cap V_{q_x} = \{\mathbf{m}^{x-}\} \tag{113}$$

$$L \cap V_{q_x+w} = \{\mathbf{m}^{x+}\} \tag{114}$$

$$L \cap H_{q_y} = \{\mathbf{m}^{y-}\} \tag{115}$$

$$L \cap H_{q_y+w} = \{\mathbf{m}^{y+}\} \tag{116}$$

with the convention that $\mathbf{m}^{x-} = (m_x^{y-}, -\infty)$ and $\mathbf{m}^{x+} = (m_x^{y+}, +\infty)$ if L is colinear to V_{q_x} and V_{q_x+w} and $\mathbf{m}^{y-} = (-\infty, m_y^{x-})$ and $\mathbf{m}^{y+} = (+\infty, m_y^{x+})$ if L is colinear to H_{q_y} and H_{q_y+w}. The segment associated to L is then

$$Q(L) = \tag{117}$$
$$[(\max\{m_x^{x-}, m_x^{y-}\}, \max\{m_y^{x-}, m_y^{y-}\}), (\min\{m_x^{x+}, m_x^{y+}\}, \min\{m_y^{x+}, m_y^{y+}\})]$$

For the sake of concision, a 0-face $\mathfrak{f}_0$ will be also noted as $\langle \mathbf{h} \rangle$ where $\mathbf{h}$ is the point that defines this face, i.e. the intersection point of these two lines.

Let L_1, L_2 be two lines of two distinct subsets of $\mathscr{V}_\Delta(Q)$, $\mathscr{H}_\Delta(Q)$, $\mathcal{A}(\mathscr{V}_\Delta)(Q)$ or $\mathcal{A}(\mathscr{H}_\Delta)(Q)$. If $L_1 \cap L_2 = \{\mathbf{h}\}$ (i.e. if $L_1 \cap L_2 \neq \emptyset$ and $L_1 \neq L_2$, i.e. L_1, L_2 are non-colinear), then $\langle \mathbf{h} \rangle$ is a 0-face of $\mathbb{H}_0(Q)$ iff $\mathbf{h} \in Q(L_1)$ and $\mathbf{h} \in Q(L_2)$. The exhaustive scanning of all the couples of lines within $\mathscr{V}_\Delta(Q)$, $\mathscr{H}_\Delta(Q)$, $\mathcal{A}(\mathscr{V}_\Delta)(Q)$ or $\mathcal{A}(\mathscr{H}_\Delta)(Q)$ then allows us to build $\mathbb{H}_0(Q)$.

A.6 Definition of $\mathbb{H}_1(Q)$

For each line L of $\mathscr{V}_\Delta(Q)$, $\mathscr{H}_\Delta(Q)$, $\mathcal{A}(\mathscr{V}_\Delta)(Q)$ or $\mathcal{A}(\mathscr{H}_\Delta)(Q)$, we keep track of all the 0-faces of $\mathbb{H}_0(Q)$ induced by the intersection of L with another line. In particular, we note $I(L)$ the sets of all the points corresponding to these 0-faces.

For the sake of concision, a 1-face $\mathfrak{f}_1$ will be also noted as $\langle \mathbf{h}_1, \mathbf{h}_2 \rangle$ where $\mathfrak{f}_1 =]\mathbf{h}_1, \mathbf{h}_2[$.

Let $I(L) = \{\mathbf{h}_0, \ldots, \mathbf{h}_i \ldots, \mathbf{h}_t\}$ ($t \geq 0$). Without loss of generality, we assume that the points $\mathbf{h}_i$ are sorted in the lexicographic order in $\mathbb{Q}^2$. (Note that we have $\mathbf{h}_0$ and $\mathbf{h}_t$ equal to the bounds of $Q(L)$.) Then, for any $0 \leq i \leq t-1$, $\langle \mathbf{h}_i, \mathbf{h}_{i+1} \rangle$ is a 1-face of $\mathbb{H}_1(Q)$. Reversely, each 1-face of $\mathbb{H}_1(Q)$ satisfies this property for one (or two) line(s) L of $\mathscr{V}_\Delta(Q)$, $\mathscr{H}_\Delta(Q)$, $\mathcal{A}(\mathscr{V}_\Delta)(Q)$ or $\mathcal{A}(\mathscr{H}_\Delta)(Q)$.

For any 1-face $\mathfrak{f}_1 = \langle \mathbf{h}_i, \mathbf{h}_{i+1} \rangle$, the set $C_0(\mathfrak{f}_1)$ is defined as $\{\langle \mathbf{h}_i \rangle, \langle \mathbf{h}_{i+1} \rangle\}$. Reversely, for any 0-face $\mathfrak{f}_0 \in \mathbb{H}_0$, the set $S_1(\mathfrak{f}_0)$ is defined as $\{\mathfrak{f}_1 \in \mathbb{H}_1 \mid \mathfrak{f}_0 \in C_0(\mathfrak{f}_1)\}$.

A.7 Definition of $\mathbb{H}_2(Q)$

Let $\mathfrak{f}_0 = \langle \mathbf{h} \rangle$ be a 0-face of $\mathbb{H}_0$. The set $S_1(\mathfrak{f}_0)$ contains many 1-faces $\langle \mathbf{h}, \mathbf{h}' \rangle$ that can be easily sorted in the clockwise order with respect to the orientation of the vectors $\mathbf{h}' - \mathbf{h}$. For each 1-face $\mathfrak{f}_1 = \langle \mathbf{h}, \mathbf{h}' \rangle$ of $\mathbb{H}_1$, we can then define the successor of $\mathfrak{f}_1$ in $S(\langle \mathbf{h} \rangle)$ (resp. in $S(\langle \mathbf{h}' \rangle)$) with respect to this ordering. This successor will be noted $\sigma(\langle \mathbf{h}', \mathbf{h} \rangle)$ (resp. $\sigma(\langle \mathbf{h}, \mathbf{h}' \rangle)$); note in particular that the order of $\mathbf{h}, \mathbf{h}'$ in the notation of σ will then be important in that case.

For the sake of concision, a 2-face $\mathfrak{f}_2$ will be also noted as $\langle \mathbf{h}_1, \ldots, \mathbf{h}_i, \ldots \mathbf{h}_t \rangle$ ($t \geq 3$) where the $\mathbf{h}_i$ are the vertices of the corresponding convex polygon, clockwise ordered. Each 2-face[6] $\mathfrak{f}_2$ is defined (up to circular permutations) by $\langle \mathbf{h}_1, \ldots, \mathbf{h}_i, \ldots \mathbf{h}_t \rangle$ such that for any $1 \leq i, j \leq t$, we have $\mathbf{h}_i \neq \mathbf{h}_j$, for any $1 \leq i \leq t-2$, we have $\sigma(\langle \mathbf{h}_i, \mathbf{h}_{i+1} \rangle) = \langle \mathbf{h}_{i+1}, \mathbf{h}_{i+2} \rangle$ and $\sigma(\langle \mathbf{h}_{t-1}, \mathbf{h}_t \rangle) = \langle \mathbf{h}_t, \mathbf{h}_1 \rangle$.

For any 2-face $\mathfrak{f}_2 = \langle \mathbf{h}_1, \ldots, \mathbf{h}_i, \ldots \mathbf{h}_t \rangle$, the sets $C_0(\mathfrak{f}_2)$ and $C_1(\mathfrak{f}_2)$ are defined as

$$C_0(\mathfrak{f}_2) = \{\langle \mathbf{h}_1 \rangle, \ldots, \langle \mathbf{h}_i \rangle, \ldots \langle \mathbf{h}_t \rangle\} \tag{118}$$

$$C_1(\mathfrak{f}_2) = \{\langle \mathbf{h}_1, \mathbf{h}_2 \rangle, \ldots, \langle \mathbf{h}_i, \mathbf{h}_{i+1} \rangle, \ldots, \langle \mathbf{h}_{t-1}, \mathbf{h}_t \rangle, \langle \mathbf{h}_t, \mathbf{h}_1 \rangle\} \tag{119}$$

Reversely, for any 0-face $\mathfrak{f}_0 \in \mathbb{H}_0$, the sets $S_1(\mathfrak{f}_0)$ and $S_2(\mathfrak{f}_0)$ are defined as

$$S_1(\mathfrak{f}_0) = \{\mathfrak{f}_2 \in \mathbb{H}_2 \mid \mathfrak{f}_0 \in C_0(\mathfrak{f}_2)\} \tag{120}$$

$$S_2(\mathfrak{f}_0) = \{\mathfrak{f}_2 \in \mathbb{H}_2 \mid \mathfrak{f}_1 \in C_1(\mathfrak{f}_2)\} \tag{121}$$

A.8 Definition of the functions $\widetilde{\phi}$, $\widetilde{\gamma}$, $\widetilde{\Phi}$, $\widetilde{\Gamma}$

Let $\mathfrak{f}_2 = \langle \mathbf{h}_1, \ldots, \mathbf{h}_i, \ldots \mathbf{h}_t \rangle$ be a 2-face of $\mathbb{H}(Q)$. We set[7]

$$\mathbf{b}(\mathfrak{f}_2) = \frac{1}{t} \sum_{i=1}^{t} \mathbf{h}_i \tag{122}$$

a point inside $\mathfrak{f}_2$, and $\mathbf{a} = \mathcal{A}^{-1}(\mathbf{b}(\mathfrak{f}_2))$. We set

$$\widetilde{\phi}(\mathfrak{f}_2) = \arg_{\mathbf{p} \in \mathbb{Z}^2} \min \|\mathbf{p} - \mathbf{b}(\mathfrak{f}_2)\| = ([b_x(\mathfrak{f}_2)], [b_y(\mathfrak{f}_2)]) \tag{123}$$

$$\widetilde{\gamma}(\mathfrak{f}_2) = \arg_{\mathbf{p} \in \mathbb{Z}^2} \min \|\mathbf{p} - \mathcal{A}^{-1}(\mathbf{b}(\mathfrak{f}_2))\| = ([a_x], [a_y]) \tag{124}$$

[6] There exists one such $\langle \mathbf{h}_1, \ldots, \mathbf{h}_i, \ldots \mathbf{h}_t \rangle$ which is not a 2-face, and that corresponds to the boundary of $\mathbb{H}(Q)$. It is characterized by the fact that it contains the four points $\mathbf{q}^{0,0}$, $\mathbf{q}^{w,0}$, $\mathbf{q}^{0,w}$ and $\mathbf{q}^{w,w}$.

[7] In practice, considering any 3 points $\mathbf{h}_i$ would be enough for our purpose.

where $[\cdot]$ is the rounding operator. From $\widetilde{\phi}$ and $\widetilde{\gamma}$, we then define $\widetilde{\Phi}$: $\widetilde{\phi}(\mathbb{H}_2) \subset \mathbb{Z}^2 \to 2^{\mathbb{H}_2}$ and $\widetilde{\Gamma} : \mathsf{S} \subset \mathbb{Z}^2 \to 2^{\mathbb{H}_2}$.

In particular, these functions allow us to define the two functions $\widetilde{\Phi} : \widetilde{\phi}(\mathbb{H}_2) \subset \mathbb{Z}^2 \to 2^{\mathbb{H}_2}$ and $\widetilde{\Gamma} : \mathsf{S} \subset \mathbb{Z}^2 \to 2^{\mathbb{H}_2}$ as follows

$$\forall \mathbf{p} \in \boxdot(Q), \forall \mathfrak{f}_2 \in \mathbb{H}_2, \mathfrak{f}_2 \in \widetilde{\Phi}(\mathbf{p}) \Leftrightarrow \widetilde{\phi}(\mathfrak{f}_2) = \mathbf{p} \tag{125}$$

$$\forall \mathbf{p} \in \mathsf{S}, \forall \mathfrak{f}_2 \in \mathbb{H}_2, \mathfrak{f}_2 \in \widetilde{\Gamma}(\mathbf{p}) \Leftrightarrow \widetilde{\gamma}(\mathfrak{f}_2) = \mathbf{p} \tag{126}$$